


Review

# Optical Crystals for 1.3 $\mu\text{m}$ All-Solid-State Passively Q-Switched Laser

Yanxin Shen <sup>1,2</sup>, Xinpeng Fu <sup>1</sup>, Cong Yao <sup>1,2</sup>, Wenyuan Li <sup>1,2</sup>, Yubin Wang <sup>1</sup>, Xinrui Zhao <sup>1,2</sup> , Xihong Fu <sup>1,\*</sup> and Yongqiang Ning <sup>1</sup>

<sup>1</sup> State Key Laboratory of Luminescence and Applications, Changchun Institute of Optics, Fine Mechanics and Physics, Chinese Academy of Sciences, Changchun 130033, China; shenyanxin20@163.com (Y.S.); fuxp@ciomp.ac.cn (X.F.); yaocong@ucas.ac.cn (C.Y.); liwenyuan@ucas.ac.cn (W.L.); wangyb@ciomp.ac.cn (Y.W.); zhaoxinrui@ucas.ac.cn (X.Z.); ningyq@ciomp.ac.cn (Y.N.)

<sup>2</sup> University of Chinese Academy of Sciences, Beijing 100049, China

\* Correspondence: fuxh@ciomp.ac.cn

**Abstract:** In recent years, optical crystals for 1.3  $\mu\text{m}$  all-solid-state passively Q-switched lasers have been widely studied due to their eye-safe band, atmospheric transmission characteristics, compactness, and low cost. They are widely used in the fields of high-precision laser radar, biomedical applications, and fine processing. In this review, we focus on three types of optical crystals used as the 1.3  $\mu\text{m}$  laser gain media: neodymium-doped vanadate (Nd:YVO<sub>4</sub>, Nd:GdVO<sub>4</sub>, Nd:LuVO<sub>4</sub>, neodymium-doped aluminum-containing garnet (Nd:YAG, Nd:LuAG), and neodymium-doped gallium-containing garnet (Nd:GGG, Nd:GAGG, Nd:LGGG). In addition, other crystals such as Nd:KGW, Nd:YAP, Nd:YLF, and Nd:LLF are also discussed. First, we introduce the properties of the abovementioned 1.3  $\mu\text{m}$  laser crystals. Then, the recent advances in domestic and foreign research on these optical crystals are summarized. Finally, the future challenges and development trend of 1.3  $\mu\text{m}$  laser crystals are proposed. We believe this review will provide a comprehensive understanding of the optical crystals for 1.3  $\mu\text{m}$  all-solid-state passively Q-switched lasers.

**Keywords:** optical crystals; 1.3  $\mu\text{m}$  laser; passively Q-switched laser; all-solid-state-laser; saturable absorber



**Citation:** Shen, Y.; Fu, X.; Yao, C.; Li, W.; Wang, Y.; Zhao, X.; Fu, X.; Ning, Y. Optical Crystals for 1.3  $\mu\text{m}$  All-Solid-State Passively Q-Switched Laser. *Crystals* **2022**, *12*, 1060. <https://doi.org/10.3390/cryst12081060>

Academic Editor: Chunhui Yang

Received: 6 July 2022

Accepted: 23 July 2022

Published: 29 July 2022

**Publisher's Note:** MDPI stays neutral with regard to jurisdictional claims in published maps and institutional affiliations.



**Copyright:** © 2022 by the authors. Licensee MDPI, Basel, Switzerland. This article is an open access article distributed under the terms and conditions of the Creative Commons Attribution (CC BY) license (<https://creativecommons.org/licenses/by/4.0/>).

## 1. Introduction

Q-switched technology is used to compress the laser energy to a narrow pulse to improve the peak power of the output laser beam. Passive Q-switched technology uses a saturable absorber (SA) as the Q-switched device to obtain output laser pulses. Since the emergence of the laser diode (LD) in the 1980s, diode-pumped solid-state laser (DPSSL) has developed rapidly owing to the achievement of narrow pulse width, high peak power, compact cavity structure, high efficiency, and low cost.

In recent years, laser radar has been extensively researched for its use in unmanned driving technology. According to the ANSI Z136.1—2014 standard, the allowable power of the 1.34  $\mu\text{m}$  laser is 1.9 times that of the 1.5  $\mu\text{m}$  and 18 times that of the 910 nm laser in the range of Class 1 power. Hence, the 1.3  $\mu\text{m}$  laser radar can output greater power and realize remote eye-safe detection. In addition, due to the low loss and low dispersion characteristics of the 1.3  $\mu\text{m}$  wavelength in the fiber, it has been widely used in the fields of communication and biosensing, for example, in the generation of non-classical optical field [1], spectral detection [2], and remote sensing [3]. Further, the 1.3  $\mu\text{m}$  wavelength laser can be used as a light source to obtain a variety of wavelength lasers through nonlinear changes such as frequency doubling [4], frequency quadrupling [5], sum frequency generation [6], and Raman scattering [7]. Thus, the 1.3  $\mu\text{m}$  passive Q-switched laser has immense application prospects in Figure 1.

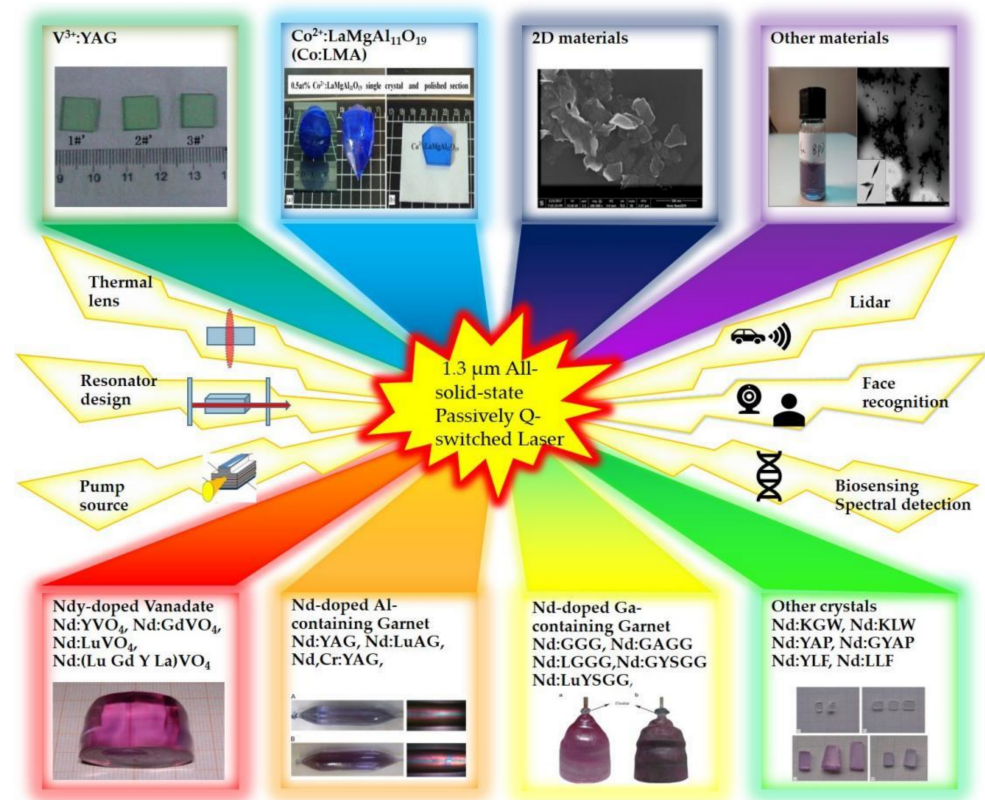


**Figure 1.** Composition and application of 1.3  $\mu\text{m}$  passively Q-switched laser. V:YAG samples [8],  $\text{Co}^{2+}:\text{LaMgAl}_{11}\text{O}_{19}$  crystal and polished section [9], SEM image of  $\text{MoS}_2\text{-SA}$  [10], Photograph of gold nanopipyramids solution and TEM image of the gold nanopipyramids [11], Nd:YVO<sub>4</sub> crystals samples [12], Nd:YAG crystals samples [13], Nd:GGG crystals samples [14], Nd:KGW crystals samples [15].

The laser gain medium as the core component of a solid-state laser is the basis for laser development.  $\text{Nd}^{3+}$  is the earliest applied doped ion, and its energy level structure is the decisive factor for the spectral characteristics of the gain medium. The substrate significantly affects the mechanical, physical, and chemical properties of the gain medium. Presently, crystal, ceramic, or glass is widely used as the substrate. The central wavelengths of radiation for these materials are generally 0.9  $\mu\text{m}$ , 1.06  $\mu\text{m}$ , and 1.3  $\mu\text{m}$ , which are derived from three energy levels transitions of  ${}^4\text{F}_{3/2}\text{-}{}^4\text{I}_{9/2}$ ,  ${}^4\text{F}_{3/2}\text{-}{}^4\text{I}_{11/2}$ , and  ${}^4\text{F}_{3/2}\text{-}{}^4\text{I}_{13/2}$ , respectively. The gain medium materials based on an LD pump must have the following characteristics: wide absorption peak, long fluorescence lifetime, large stimulated emission cross section, good mechanical properties, and high thermal conductivity. In this review, we discuss the 1.3  $\mu\text{m}$  laser crystals, namely Nd:YVO<sub>4</sub> [16], Nd:GdVO<sub>4</sub> [17], Nd:YAG [18], Nd:GGG [19], Nd:KGW [20], Nd:YAP [21]. Among them, Nd:YVO<sub>4</sub>, Nd:GdVO<sub>4</sub>, and Nd:YAG are the major gain medium materials that can obtain high repetition rate and large output power. In 2015 Nikkinen et al. [22] reported a 1.3  $\mu\text{m}$  Nd:YVO<sub>4</sub> microchip laser with a dilute nitride GaInNAs/GaAs saturable absorber mirror. The laser produced pulse as narrow as 204 ps with 2.3 MHz repetition rate. In 2015 Wang et al. [23] realized a high-peak-power (64.9 kW), short-pulse-width (6.16 ns) passively Q-switched Nd:YAG/V<sup>3+</sup>:YAG laser at 1.3  $\mu\text{m}$ . In 2019 Li et al. [24] simultaneously used both V<sup>3+</sup>:YAG and  $\text{MoSe}_2$  SA as passively Q-switched device. The pulse duration was 82.4 ns pulse at a repetition rate of 409.3 kHz. During the recent decades, researchers have created new optical crystals such as Nd:(Lu Gd Y La) VO<sub>4</sub> mixed crystal [25], Nd,Cr:YAG double-doped crystal [26,27], Nd:GYSGG crystal [28–30] and so on. In 2009 Huang et al. [31] investigated a diode-end-pumped passively Q-switched Nd:Gd<sub>0.5</sub>Y<sub>0.5</sub>VO<sub>4</sub> laser at 1.34  $\mu\text{m}$ . For the passive Q-switching operation, the narrowest pulse width was 47.8 ns with 76 kHz repetition rate, with peak power estimated to be

182 W, respectively. In 2011 Li et al. [32] realized passively Q-switched laser operation with a mixed c-cut Nd:Gd<sub>0.33</sub>Lu<sub>0.33</sub>Y<sub>0.33</sub>VO<sub>4</sub> crystal at 1.34 μm. For passively Q-switched operation, the narrowest pulse width of 26 ns, the highest peak power of 1.8 kW were obtained using V:YAG as Q-switch. In 2016, Lin et al. [33] used Nd,Cr:YAG as gain medium and V<sup>3+</sup>:YAG as SA to achieve dual-wavelength output (946 nm, 1.3 μm). The maximum average output power of 1.3 μm laser was 0.6 W, the narrowest pulse width was 19.2 ns at the highest repetition rate of 43.25 kHz. In 2017 Lin et al. employed a Co:MgAl<sub>2</sub>O<sub>4</sub> crystal in a Nd:GYSGG passively Q-switched laser. The narrowest pulse width of 20.5 ns was achieved. The highest peak power was 1319 W under a pump power of 7.20 W, respectively. They provide the basis for further improving the output performance of the laser.

SA is considered an important part of a passively Q-switched laser. It utilizes the saturable absorption effect to modulate the loss in the laser cavity for realizing the Q-switching process. V<sup>3+</sup>:YAG [8] and Co<sup>2+</sup>:LaMgAl<sub>11</sub>O<sub>19</sub> (Co:LMA) [9] are the most commonly used in the 1.3 μm band. Their ratios of the excited-state absorption cross section to the ground-state absorption cross section are approximately 0.1 and 0.2, respectively. Moreover, their ground-state recovery time is relatively short; hence, they are easily bleached. When these two materials were used in Q-switched devices, the pulse peak power was above 330 kW [34] and pulse width could reach 1 ns [35]. Further, the output repetition rate of 1820 kHz could be obtained [35]. In recent years, with the rapid development of new materials and nanotechnology, some new SA devices have emerged [36], such as graphene [37–45], black phosphorus [46,47], topological insulators (TI) [48,49], transition metal disulfides (TMDs) [10,24,50–56], gold nanomaterials [11,57], MXene [58–60], and so on. Most novel SA devices have been reported to achieve high-repetition-rate pulse output (>150 kHz) but large pulse width (>60 ns) and low peak power (<30 W). Owing to the development of SA materials, the performance of passively Q-switched lasers is expected to be further improved.

In this review, we first classify the 1.3 μm laser crystals and introduce their properties. Next, we focus on the research progress of different types of 1.3 μm passively Q-switched laser and reveal the development bottleneck for 1.3 μm laser crystals. In addition, we also introduce some new optical crystals and novel SA materials. Finally, we summarize the study and discuss the scope for future development of 1.3 μm laser crystals.

## 2. Classification of 1.3 μm Laser Crystals

### 2.1. Neodymium-Doped Vanadate

As the most popular 1.3 μm laser crystals, the Nd-doped vanadate crystals mainly include Nd:YVO<sub>4</sub>, Nd:GdVO<sub>4</sub>, Nd:LuVO<sub>4</sub>, and Nd:Y<sub>x</sub>Gd<sub>1-x</sub>VO<sub>4</sub> (x = 0–1). Among them, Nd:YVO<sub>4</sub> and Nd:GdVO<sub>4</sub> have been widely researched.

Nd:YVO<sub>4</sub> is an excellent laser crystal with mature technology. It was first invented by O'Connor [61] of the MIT Lincoln Laboratory. It is a natural birefringence crystal with thermal conductivity of 5.2 Wm<sup>-1</sup>K<sup>-1</sup> and absorption bandwidth of approximately 20 nm. Since the stimulated emission cross section of Nd:YVO<sub>4</sub> at 1342 nm (1 at.%, 7.6 × 10<sup>-19</sup> cm<sup>2</sup> is 18 times larger than that of Nd:YAG) is smaller than the ground-state absorption cross section of a saturated absorber (V<sup>3+</sup>:YAG, 7.2 × 10<sup>-18</sup> cm<sup>2</sup>) and the upper-level lifetime is short (98 μs) [62], the Nd:YVO<sub>4</sub> laser can achieve high-repetition-rate pulses output. As early as 1976, Toker et al. [63] realized a 1.3 μm continuous-wavelength output by end-pumping Nd:YVO<sub>4</sub> with an argon-ion laser. However, the slope efficiency was only 7%.

In 1997, Fluck et al. [64] proposed a diode-pumped 1.34-μm-wavelength passively Q-switched microchip laser, and an InGaAsP semiconductor SA mirror was used as a Q-switched device. When pumped at 400 mW, the pulse repetition rate was 53 kHz and pulse width was 230 ps, but the peak power was only 450 mW. In 2005, Lai et al. [65] used the InAs/GaAs quantum dot material as an SA. When the incident pump power was 2.2 W, the output pulse repetition rate of 770 kHz, pulse width of 90 ns, and peak power of above 5 W were obtained. In 2006, Janousek et al. [66] investigated passively synchronous dual-wavelength (1064 and 1342 nm) Q-switched lasers based on V<sup>3+</sup>:YAG

SA. The schematic of this laser is shown in Figure 2. When the pump power was 3.5 W, the output laser repetition rate was 10 kHz, the pulse width was 70 ns, and the intracavity peak power was 3 kW. In 2020, Kane et al. [35] used a Nd:YVO<sub>4</sub> microchip as the gain medium, and employed V<sup>3+</sup>:YAG and output coupler (OC) mirrors with different transmittances to conduct multiple sets of experiments. In one group of experiments, the repetition rate of the output pulse was 460 kHz, pulse duration was 1.6 ns, and peak power was approximately 500 W. In another group, the repetition rate of the output pulses was 24 kHz, pulse duration was 1.08 ns, and peak power was 2.3 kW. Although only the experimental data were reported by the authors and no detailed experimental results were presented, the study provided the basis for further realizing a 1.3 μm pulse laser with narrow pulse width, high peak power, high repetition rate, and good stability.

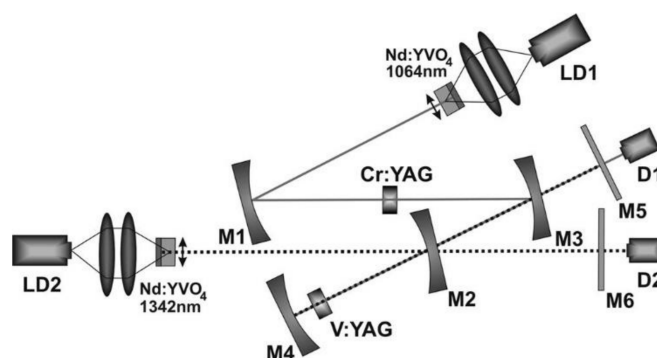


**Figure 2.** Setup for passively synchronized Q-switched Nd:YVO<sub>4</sub> lasers oscillating at 1064 and 1342 nm [66].

Nd:YVO<sub>4</sub> is a commonly used crystal, it is usually used to produce 1.3 μm wavelength laser. It has a five times higher absorption efficiency than that of Nd:YAG. The stimulated emission cross section of Nd:YVO<sub>4</sub> at 1342 nm is 18 times bigger than that of Nd:YAG at 1.3 μm, resulting in a more compact structure. Table 1 lists the research progress on the 1.3 μm Nd:YVO<sub>4</sub> laser. Using Nd:YVO<sub>4</sub> as the gain medium not only ensure a high repetition rate of several MHz, but also achieves a high peak power of several kW. In these results, V<sup>3+</sup>:YAG is considered to be an ideal SA material for Nd:YVO<sub>4</sub> at 1.3 μm.

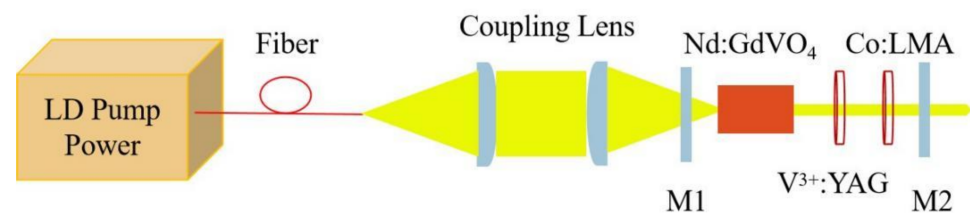
Nd:GdVO<sub>4</sub> is also a popular Nd-doped vanadate crystal which has been widely recognized as the gain medium of DPSSLs since its development by Zagumennyi et al. [17] in 1992. The structure of the Nd:GdVO<sub>4</sub> crystal is the same as that of the Nd:YVO<sub>4</sub> crystal, with a zircon structure and tetragonal system. The absorption half-width is 1.6 nm near 808 nm. The branching ratio of the 1.34 μm fluorescence spectrum to 1.06 μm is approximately 0.2, which can emit a 1.3 μm laser. It has a large stimulated emission cross section (c-cut 0.52 at.%,  $1.8 \times 10^{-19}$  cm<sup>2</sup>@1342 nm), short upper-level lifetime (100 μs), and high thermal conductivity ( $11.7 \text{ Wm}^{-1} \text{ K}^{-1}$ ), and achieves high doping concentration [25,78]. Therefore, high repetition rate and high-energy pulse output can be realized.

In 2007, Qi et al. [79] investigated an LD-pumped c-cut Nd:GdVO<sub>4</sub> crystal with a Co:LMA SA, lasing at 1.34 μm wavelength. The maximum repetition rate of the laser output was 277 kHz, shortest pulse width was 32 ns, output power was 266 mW, and maximum peak power was 187 W. In 2008, Ma et al. [34] compared the output characteristics of a-cut and c-cut Nd:GdVO<sub>4</sub> passively Q-switched lasers at 1342 nm. When the pump energy of the flash lamp was 27 J, the corresponding output laser pulse width of the two crystals were 61.72 ns and 53.94 ns, and the single pulse output energies were 15.5 mJ and 17.6 mJ, respectively. The corresponding peak powers were 247 kW and 330 kW. In 2011, Li et al. [80] simultaneously used V<sup>3+</sup>:YAG and Co:LMA SA in the cavity to obtain a narrower pulse width and higher peak power. The schematic of this laser is shown in Figure 3. The corresponding output laser repetition frequencies were 49.8 kHz and 36 kHz, pulse widths were 16.9 ns and 11.3 ns, maximum average output powers were 0.319 W and 0.268 W, and peak powers were 378.2 W and 659 W.

**Table 1.** Research progress on 1.3  $\mu\text{m}$  passively Q-switched Nd:YVO<sub>4</sub> lasers.

Year	C <sub>Nd</sub>	Nd:YVO <sub>4</sub>						Ref.
		SA	T <sub>oc</sub>	P <sub>Ave</sub> (W)	Pulse Width (ns)	Peak Power (W)	Repetition Rate (kHz)	
1997	3 at. %	InGaAsP	8.5%	0.0065	0.23	0.45	53	[64]
2003	1 at. %	PbS (T = 97%)	3%	0.012	110	-	295	[67]
		V <sup>3+</sup> :YAG (T = 95%)	8%	0.023	200	-	250	
2005	2 at. %	InAs/GaAs	5%	0.013	13	150	7	[65]
2005	1 at. %	V <sup>3+</sup> :YAG (T = 85%)	6%	0.36	90	>5	770	[62]
2006	1 at. %	V <sup>3+</sup> :YAG (T = 90%)	7%	0.096	8.8	436	25	[66]
2006	0.5 at. %	InGaAsP	-	-	70	3000 (intra)	10	[68]
2007	0.27 at. %	Co <sup>2+</sup> :LMA (T = 90%)	6%	0.16	19	220	38	[69]
2011	0.3 at. %	V <sup>3+</sup> :YAG (T = 94%)	9.7%	0.58	42	346	40	[70]
2011	0.5 at. %	nc-Si/SiN <sub>x</sub> film	3%	0.9	54	180	89	[71]
2015	Microchip	GaInNAs/GaAs	8%	0.67	51	~592	22.2	[22]
2017	0.4 at. %	Graphene oxide	5%	0.024	0.204	-	2300	[44]
2018	YVO <sub>4</sub> /Nd:YVO <sub>4</sub> /YVO <sub>4</sub>	MXene Ti <sub>3</sub> C <sub>2</sub> T <sub>x</sub>	5%	0.52	329	7.39	214	[58]
2018	0.4 at. %	Antimonene	4%	0.03	454	0.406	162	[72]
2019	0.1 at. %	Bi:GaAs	5%	0.039	48.33	28.17	28.65	[73]
		GaAs	3.8%	0.435	64	48.7	138	
2019	YVO <sub>4</sub> /Nd:YVO <sub>4</sub> /YVO <sub>4</sub> (0.3 at. %)	WS <sub>2</sub>	4%	0.405	282	~9	158	[55]
2019	YVO <sub>4</sub> /Nd:YVO <sub>4</sub> /Nd:YVO <sub>4</sub> 0 at.%0.1 at%0.3 at%	MoS <sub>2</sub>	12%	0.538	550	10.1	97	[10]
		V <sup>3+</sup> :YAG (T = 97.5%)	4%	-	4.8	89	1820	
		V <sup>3+</sup> :YAG (T = 97.5%)	4%	-	6.4	144	680	
		V <sup>3+</sup> :YAG (T = 95%)	4%	-	2.2	344	616	
		V <sup>3+</sup> :YAG (T = 95%)	4%	-	3.6	383	295	
		V <sup>3+</sup> :YAG (T = 90%)	4%	-	1.6	500	460	
		V <sup>3+</sup> :YAG (T = 90%)	14%	-	1.6	2400	93	
2020	Microchip	V <sup>3+</sup> :YAG (T = 79%)	4%	-	1.3	2500	11	[35]
		V <sup>3+</sup> :YAG (T = 79%)	4%	-	1.08	2300	24	
		PtSe <sub>2</sub>	5%	0.209	775	2.61	103.5	
		GO-FONP	10%	0.306	163	5.98	314	
		FONP	5%	0.14	767	1.56	116	
		GaInSn	10%	0.425	32	1622	44	
		Ti <sub>3</sub> C <sub>2</sub> (OH) <sub>2</sub> /Ti <sub>3</sub> C <sub>2</sub> F <sub>2</sub>	3%	0.48	390	6.25	195	
2020	0.5 at. %	Mo <sub>2</sub> C	5%	0.236	222	4.5	236	[56]
2020	0.3 at. %	Mo <sub>2</sub> C	5%	0.293	313	10.04	93	[60]
2020	0.5 at. %	Mo <sub>2</sub> C	5%	0.293	313	10.04	93	[60]
2022	-	Ti <sub>2</sub> C Mxene	-	0.215	190	7.75	146	[77]

C<sub>Nd</sub>, Nd doping concentration; T<sub>oc</sub>, transmission of output coupler mirror; P<sub>Ave</sub>, average output power; GO-FONP, graphene oxide and ferroferric-oxide nanoparticle hybrid.

**Figure 3.** Experimental setup [80].

The Nd:GdVO<sub>4</sub> crystal has large stimulated emission cross section and short upper-level lifetime, which ensures high repetition rate, short pulse width, and peak power. Table 2 summarizes the research progress on the 1.3  $\mu\text{m}$  Nd:GdVO<sub>4</sub> laser. Compared with the single SA, the pulse width was greatly reduced and peak power was increased by using double SA as the Q-switched device. However, additional losses were introduced, which decreased the output power. Composite crystals with different doping concentrations can enhance the absorption of pump light, thereby increasing the output power. V<sup>3+</sup>:YAG and Co<sup>2+</sup>:LMA crystals are ideal SAs for the Nd:GdVO<sub>4</sub> crystal. Although the use of two-dimensional materials such as bismuth quantum dots and TMDs as SAs yields high-repetition-rate output (>100 kHz), the pulse width (>80 ns) and peak power (<10 W) are not satisfactory.

**Table 2.** Research progress on 1.3  $\mu\text{m}$  passively Q-switched Nd:GdVO<sub>4</sub> lasers.

Nd:GdVO <sub>4</sub>								
Year	C <sub>Nd</sub>	SA	T <sub>OC</sub>	P <sub>Ave</sub> (W)	Pulse Width (ns)	Peak Power (W)	Repetition Rate (kHz)	Ref.
2007	0.52 at.% c-cut	Co <sup>2+</sup> :LMA (T = 90%)	5.5%	0.266	32	187	277	[79]
2008	0.52 at.% a-cut c-cut	V <sup>3+</sup> :YAG (T = 54%)	10%	-	61.72	247,000	-	[34]
			3%	0.519	-	-	-	
2009	0.52 at.% a-cut c-cut	V <sup>3+</sup> :YAG (T = 94%)	10%	0.441	-	-	-	[81]
			3%	-	21.7	307	48.41	
2010	0.5 at.% a-cut	V <sup>3+</sup> :YAG (T = 96%)	15%	0.782 *	80	244	53.25	[82]
2011	0.5 at.% c-cut	Co <sup>2+</sup> :LMA +V <sup>3+</sup> :YAG (T = 94%) (T = 90%) +V <sup>3+</sup> :YAG (T = 50%)	5%	0.319	16.9	378.2	49.8	[80]
2018	0.5 at.%	Au-NBPs (T = 90%)	4%	0.175	342	3.6	141.8	[11]
2018	0.3 at.% a-cut	Black phosphorus	8%	0.452	77	10.04	625	[47]
2018	-	1T-TiSe <sub>2</sub>	15%	0.36	344	4.67	224	[51]
		MoSe <sub>2</sub>		0.0526	420	0.52565	238	
2019	c-cut composite crystal 0.1 at.%/0.3 at.%/0.8 at.%	V <sup>3+</sup> :YAG+MoSe <sub>2</sub> V <sup>3+</sup> :YAG	3.8%	0.1922 0.04	82.4 267	5.6 -	409.3 -	[24]
2019	c-cut composite crystal 0.1 at.%/0.5 at.%/1 at.%	ZIF-67	3.8%	0.109	108	2.43	415	[83]
2019	0.5 at.%	BiQDs	5%	0.125	510	1.8	135	[84]
2020	c-cut composite crystal 0.1 at.%/0.3 at.%/0.8 at.%	BiQDs	3.8%	0.12	155	1.68	457	[85]
2020	-	ITO-NWAs	10%	0.32	296	4.69	230.2	[86]
2021	-	Co <sup>2+</sup> : $\beta$ -Ga <sub>2</sub> O <sub>3</sub>	3.8%	0.035	280	-	181	[87]
2021	0.3 at.%	$\alpha$ -Fe <sub>2</sub> O <sub>3</sub> nanosheets	3.8%	0.114	180	1.8	358	[88]
2022	1 at.%	m-BiVO <sub>4</sub>	3.8%	0.1153	355	1.35	242.6	[89]

C<sub>Nd</sub>, Nd doping concentration; T<sub>OC</sub>, transmission of output coupler mirror; P<sub>Ave</sub>, average output power; Au-NBPs, gold nanobipyramids; ZIF-67, zeolitic imidazolate framework-67; BiQDs, bismuth quantum dots; ITO-NWAs, broadband indium tin oxide nanowire arrays. m-BiVO<sub>4</sub>, monoclinic bismuth vanadate.

In 2002, Maunier et al. [90] obtained Nd:LuVO<sub>4</sub> by replacing yttrium with lutetium. The stimulated emission cross section of the c-cut Nd:LuVO<sub>4</sub> at 1.34  $\mu\text{m}$  was  $1.5 \times 10^{-19} \text{ cm}^2$  ( $\pi$  polarization) and  $1.9 \times 10^{-19} \text{ cm}^2$  ( $\sigma$  polarization), with high thermal conductivity ( $9.77 \text{ W m}^{-1} \text{ K}^{-1}$ ) and small upper energy lifetime (95  $\mu\text{s}$ ) [90–92]. Liu et al. [93] reported a diode-pumped passively Q-switched Nd:LuVO<sub>4</sub> laser at 1.34  $\mu\text{m}$  in 2008. The maximum output peak power of 820 W was attained with the pulse repetition rate of 22.4 kHz. In 2010, Liu et al. [94] used Co:LMA as the SA to obtain 534 kHz high-repetition-rate pulse output with an 8% transmission OC mirror.

Usually, a series of Nd:(Lu Gd Y La)VO<sub>4</sub> mixed crystals is grown by combining two ions, which is very suitable as the gain medium of Q-switched lasers owing to the long upper-energy-level life and small stimulated emission cross section [25]. For example, Nd:Y<sub>x</sub>Gd<sub>1-x</sub>VO<sub>4</sub> ( $x = 0\sim 1$ ) crystals were successfully grown by the Czochralski method. The thermal conductivity, specific heat capacity, and stimulated emission cross section of Nd:Y<sub>x</sub>Gd<sub>1-x</sub>VO<sub>4</sub> were different owing to the different crystal composition ratio, Nd ion doping, and cutting direction. For example, when  $x = 0.37, 0.63$ , the corresponding specific heat capacities of Nd:Y<sub>x</sub>Gd<sub>1-x</sub>VO<sub>4</sub> are 28.33 and 28.98  $\text{cal mol}^{-1} \text{ K}^{-1}$ , and the thermal conductivities are  $4.88 \text{ W m}^{-1} \text{ K}^{-1}$  and  $5.04 \text{ W m}^{-1} \text{ K}^{-1}$ , respectively [95]. Taking the Nd:Gd<sub>0.5</sub>Y<sub>0.5</sub>VO<sub>4</sub>/V<sup>3+</sup>:YAG laser as an example, the stimulated emission cross section of the gain medium is  $1.0 \times 10^{-19} \text{ cm}^2$ , ground-state absorption cross section is  $7.2 \times 10^{-18} \text{ cm}^2$  at 1.3  $\mu\text{m}$ , and V<sup>3+</sup>:YAG ground-state absorption cross section is  $7.2 \times 10^{-18} \text{ cm}^2$ ; hence, the second threshold conditions are easily achieved [31]. Therefore, the Nd:(Lu Gd Y La) VO<sub>4</sub> crystals can achieve 1.3- $\mu\text{m}$ -wavelength high-repetition-rate pulse laser output [31,32,96–99].

In 2010, Omatsu et al. [97] demonstrated an LD side-pumped bounce amplification laser with a slab of Nd:Gd<sub>0.6</sub>Y<sub>0.4</sub>VO<sub>4</sub> crystal as the gain medium and V:YAG as the SA. The maximum output power of 6.5 W and peak power of 0.87 kW were obtained at the pump power of 37 W, pulse laser repetition rate of 150 kHz, and pulse width of approximately 50 ns.

In 2011, Li et al. [100] investigated the laser performance with a mixed Nd:Lu<sub>0.15</sub>Y<sub>0.85</sub>VO<sub>4</sub> crystal at 1.34  $\mu\text{m}$  wavelength. When V<sup>3+</sup>:YAG T<sub>0</sub> = 89%, pulses with repetition rate of 42.5 kHz, minimum pulse width of 30.6 ns, and peak power of 268 W were obtained. When

$T_0 = 96\%$ , the pulse repetition rate was 248 kHz, pulse width was 83.4 ns, and peak power was 21.6 W. In 2022, Cai et al. [101] prepared a tin disulfide saturable absorber. A stable passively Q-switched (PQS) Nd:Lu<sub>0.15</sub>Y<sub>0.85</sub>VO<sub>4</sub> 1.3  $\mu$ m laser was successfully realized. It had a repetition rate of 1.18 MHz, the shortest pulse width of 34 ns, and a peak power of 20.8 W. In another work Cai et al. [102] successfully fabricated a nickel-cobalt layered double hydroxide SA, and it was used as a passively mode-locked modulator for the first time. It could obtain stable pulse sequence with a repetition frequency of 1.18 MHz and a narrowest pulse width of 52 ns, the corresponding peak power was 13.89 W. The experimental device is shown in Figure 4.

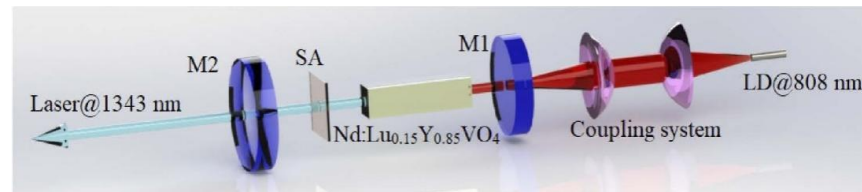


**Figure 4.** Passively Q-switched 1.34  $\mu$ m laser experimental device with nickel-cobalt layered double hydroxide SA [102].

In 2013, Han et al. [103] proposed a Nd:La<sub>0.05</sub>Lu<sub>0.95</sub>VO<sub>4</sub> crystal as the gain medium to produce pulse laser with repetition rate of 33 kHz, average output power of 0.19 W, pulse width of 41 ns, and peak power of 199 W.

## 2.2. Neodymium-Doped Aluminum-Containing Garnet

Nd:YAG is a commonly used laser crystal. Geusic et al. [18] fabricated the Nd:YAG crystal output laser for the first time in 1964. The thermal conductivity of Nd:YAG is  $14 \text{ W m}^{-1} \text{ K}^{-1}$ , specific heat is  $0.59 \text{ J/g K}$ , stimulated emission cross sections are  $0.8 \times 10^{-19} \text{ cm}^2$  (1319 nm) and  $0.9 \times 10^{-19} \text{ cm}^2$  (1338 nm), Mohs hardness is 8.5, absorption line width is 4 nm, and fluorescence lifetime is 230  $\mu$ s [104]. Hence, the Nd:YAG laser can achieve high repetition rate and peak power pulse output at 1.3  $\mu$ m wavelength.

In 2006, Jabczynski et al. [105] used a 600 W diode-stack side-pumped triangular Nd:YAG slab laser to achieve pulse width of 6 ns, peak power of 125 kW, and passively Q-switched pulse output at 1.3  $\mu$ m wavelength. The schematic is displayed in Figure 5. In 2011, Li et al. [106] realized the passive Q-switched output of Nd:YAG at 1319 nm with V<sup>3+</sup>:YAG SA. When the transmittance of the OC mirror was 2.8%, the repetition rate of the output pulse laser was 230 kHz and minimum pulse width was 128 ns. In 2016 Lin et al. [107] pumped Nd:YAG with 885 nm LD to obtain dual-wavelength output laser at 1319 nm and 1338 nm. The shortest pulse widths are 20.20 ns and 20.86 ns, respectively. The maximum repetition rate is 64.10 kHz.

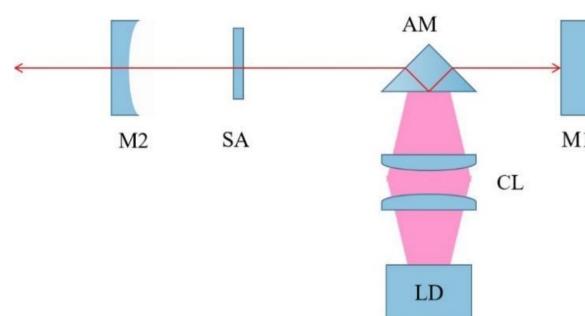


**Figure 5.** Arrangement of the laser resonator with side-pumped trigonal crystal (LD, fast-collimated pumping laser diode; CL, coupling lens; AM, triangular slab active medium; SA, V:YAG; M2, laser output coupler; M1, laser rear mirror).

In 2018, Zhou et al. [4] experimentally demonstrated a passively Q-switched red laser with an Nd<sup>3+</sup>:YAG/YAG/V<sup>3+</sup>:YAG/YAG composite crystal. This work first achieved

1327.6 nm laser and its second harmonic generation from the Nd<sup>3+</sup>:YAG. In 2019, Lin et al. [52] prepared ReS<sub>2</sub> by liquid phase exfoliation method. For the first time, it was used as passively Q-switched devices at 1.3 μm wavelength. The repetition rate of the output pulse laser reached 214 kHz, pulse width was 403 ns, maximum average output power was 78 mW, and pulse peak power was 0.9 W. The schematic is displayed in Figure 6.

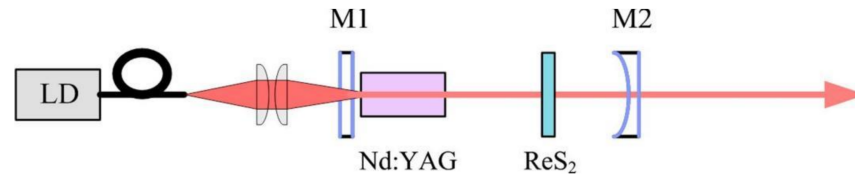


**Figure 6.** The schematic of Q-switched laser cavity based on ReS<sub>2</sub> SA. M1: plane input mirror; M2: concave output mirror with radius of  $-100$  mm and 8% transmittance [52].

Table 3 lists the research progress on the 1.3 μm Nd:YAG laser, in which the combination of Nd:YAG and V<sup>3+</sup>:YAG demonstrated high repetition rate, peak power, narrow pulse width, and passively Q-switched pulse output at 1.3 μm wavelength. When two-dimensional materials such as graphene and metal disulfide were used as the SA, the pulse width of the high-repetition-frequency pulse output laser was more than 100 ns and peak power was less than 20 W. In the experiment, a composite crystal such as YAG/Nd:YAG/V:YAG could shorten the cavity length and enhance the heat dissipation, thereby shortening the pulse width and improving the average output power and peak power. The Nd:YAG laser could also improve the output power through the dual-wavelength (1319, 1338 nm) output.

**Table 3.** Research progress on 1.3 μm passively Q-switched Nd:YAG lasers.

Nd:YAG									
Year	C <sub>Nd</sub>	SA	T <sub>OC</sub>	P <sub>Ave</sub> (W)	Pulse Width (ns)	Peak Power (W)	Repetition Rate (kHz)	Ref.	
2003	-	V <sup>3+</sup> :YAG (T = 95.7%)	15%	1.56	20	1200	60	[108]	
		Double V <sup>3+</sup> :YAG		0.96	20	2400	20		
		T = 89%	6%	0.215	21	3100	5.6		
2004	1 at. %	YAG/Nd:YAG (4 + 8)mm	V <sup>3+</sup> :YAG	T = 93%	9%	0.525	30	4300	11
			T = 91%	9%	0.365	25	4800	5.3	
		YAG/Nd:YAG/VYAG (4 + 8 + 0.5) mm		14%		0.5	19.7 ± 0.3	5000	5.2
			V <sup>3+</sup> :YAG (T = 88%)	9%	0.7	14.7 ± 0.5	4600	10.4	
				18%	0.43	11.0 ± 0.4	6100	6.4	
2006	Triangular Slab	V <sup>3+</sup> :YAG (T = 95.7%)	25%	-	6	125,000	-	[105]	
2007	1.1 at. %	YAG/Nd:YAG (4 + 8) mm	V <sup>3+</sup> :YAG (T = 85%)	10%	0.6	6.2 ± 0.2	6000 ± 300	15	[110]
		Nd:YAG 4 mm		0.25	1.7 ± 0.1	11,000 ± 2000	11		
2010	2 at. %		T = 89.6% (1319 nm) T = 89.7% (1338 nm)	12.5% (1319 nm) 12% (1338 nm)	0.266	15	167	133	[104]
			Co <sup>2+</sup> :LMA						
2011	0.6 at. %		V <sup>3+</sup> :YAG (T = 92%)	2.8%	1.8	128	-	230	[106]
2013	0.6 at. %		Graphene Oxide	10%	0.82	2000	11.7	35	[39]
2015	1 at. %		V <sup>3+</sup> :YAG (T = 88%)	2.5%	0.628	21	2100	15	[111]
			T = 90%	15%	3.3 mJ	-	-	77.5	[23]
2015	1.1 at. %		V <sup>3+</sup> :YAG	T = 85%	25%	2.4 mJ	6.16	64,900	34.1
2016	1 at. %		Multilayer Graphene (T = 89%)	2.5%	0.34	380	139	209	[41]
					1.97	20.2	-	-	
2016	1 at. %		V <sup>3+</sup> :YAG (T = 90%)	6%		1319 nm	-	64.1	[107]
					1.58	20.86	-	-	
						1338 nm	-	-	
2018	Nd <sup>3+</sup> :YAG/YAG/V <sup>3+</sup> :YAG/YAG		V <sup>3+</sup> :YAG	2.8%	2.41	-	-	-	[4]
	1 at. %								
2018	1.1 at. %		Co:MgAl <sub>2</sub> O <sub>4</sub> (T = 89.5%)	16%	0.48	18.3	1533	17.5	[112]
2019	1 at. %		ReS <sub>2</sub>	8%	0.078 W	403	0.9	214	[52]
2019	-		ReS <sub>2</sub>	-	0.101 W	111	2.95	308.4	[53]
2019	-		SnS <sub>2</sub>	-	0.136 W	323	1.89	223	[54]

C<sub>Nd</sub>, Nd doping concentration; T<sub>OC</sub>, transmission of output coupler mirror; P<sub>Ave</sub>, average output power; L<sub>cav</sub>, cavity length.



Nd:Lu<sub>3</sub>Al<sub>5</sub>O<sub>12</sub> (Nd:LuAG) is an isostructure of Nd:YAG, which can be used to grow high-quality single crystals. It has high thermal conductivity ( $9.6 \text{ W}\cdot\text{m}^{-1}\cdot\text{K}^{-1}$ ), large absorption cross section ( $1.52 \times 10^{-20} \text{ cm}^2$ ), and stimulated radiation cross section at  $1.3 \mu\text{m}$  of  $0.5 \times 10^{-19} \text{ cm}^2$ . The full width at half maximum (FWHM) of the absorption band (5 nm) and fluorescence lifetime (277  $\mu\text{s}$ ) are both greater than those of Nd:YAG, but the absorption coefficient is slightly lower, which is suitable for a high-repetition-rate and high-energy laser [113].

In 2015, Liu et al. [114] used V<sup>3+</sup>:YAG SA to realize Nd:LuAG  $1.3 \mu\text{m}$  passively Q-switched output with minimum pulse width of 17 ns and maximum single pulse energy of 18.9  $\mu\text{J}$ . In 2017, Wang et al. [50] realized a Nd:LuAG 99 kHz high-repetition-frequency passive Q-switched output based on MoS<sub>2</sub> SA.

### 2.3. Neodymium-Doped Gallium-Containing Garnet

Nd:Gd<sub>3</sub>Ga<sub>5</sub>O<sub>12</sub> (Nd:GGG) was first reported by Geusic et al. [18] in 1964. The stimulated emission cross section of Nd:GGG at 1331 nm is  $3.9 \times 10^{-20} \text{ cm}^2$ , fluorescence lifetime is 240  $\mu\text{s}$ , thermal conductivity is  $6.4 \text{ W}\cdot\text{m}^{-1}\cdot\text{K}^{-1}$ , specific heat capacity is  $380 \text{ J}\cdot\text{kg}^{-1}\cdot\text{K}^{-1}$ , and absorption linewidth is 4 nm. In addition, it also exhibits the advantage of yielding a large-size crystal [19], which promotes its wide application in solid-state heat capacity lasers.

In 2016, Han et al. [46] performed a passively Q-switched experiment with Nd:GGG crystal and black phosphorus SA. A pulse output with repetition rate of 175 kHz, pulse width of 363 ns, average output power of 157 mW, and peak power of 3 W was obtained.

In 2010, Zhang et al. [115] obtained a  $1.33\text{-}\mu\text{m}$ -wavelength pulsed laser by using an LD end-pumped Nd:GAGG crystal. The maximum average output power was 450 mW with a 3% transmittance of the OC mirror. The maximum peak pulse power was 7.1 kW with an 8% transmittance of the OC mirror.

In 2021, Gao et al. [116] investigated passively Q-switched Nd:LGGG lasers at  $1.3 \mu\text{m}$ . In the Q-switching regime, a repetition rate of 8 kHz with a minimum pulse duration of 9.75 ns was obtained, the corresponding peak power was 2.4 kW.

Nd:GGG crystals doped with ions such as Al<sup>3+</sup>, Y<sup>3+</sup>, and Lu<sup>3+</sup> were fabricated, which could grow a variety of new crystals such as Nd:Gd<sub>3</sub>Al<sub>x</sub>Ga<sub>5-x</sub>O<sub>12</sub> ( $x = 0.94$ ) (Nd:GAGG) [117], Nd:(Lu<sub>x</sub>Gd<sub>1-x</sub>)<sub>3</sub>Ga<sub>5</sub>O<sub>12</sub> (Nd:LGGG) [118,119], Nd:Gd<sub>3x</sub>Y<sub>3(1-x)</sub>Sc<sub>2</sub>Ga<sub>3(1+δ)</sub>O<sub>12</sub> (Nd:GYSGG) [28], and Nd:Lu<sub>3</sub>Sc<sub>1.5</sub>Ga<sub>3.5</sub>O<sub>12</sub> (Nd:LuYSGG) [120]. They can be used as a  $1.3 \mu\text{m}$  solid-state laser gain medium. Since the doped ions replace Gd<sup>3+</sup> or Ga<sup>3+</sup> in the crystals, the newly formed crystals have wider non-uniform spectrum broadening, smaller excitation cross section, and greater energy storage capacity. The research progress is detailed in Table 4.

**Table 4.** Research progress on  $1.3 \mu\text{m}$  passively Q-switched neodymium-doped gallium garnet lasers.

Year	C <sub>Nd</sub>	SA	T <sub>OC</sub>	P <sub>Ave</sub> (W)	Pulse Width (ns)	Peak Power (W)	Repetition Rate (kHz)	Ref.
Nd:Gd <sub>3</sub> Ga <sub>5</sub> O <sub>12</sub> (Nd:GGG)								
2009	1 at.%	Co <sup>2+</sup> :LMA	T = 90%	0.183	26.1	700	-	[121]
			T = 81%	0.131	16.4	1300	6.1	
2009	1 at.%	V <sup>3+</sup> :YAG (T = 94%)	8%	0.46	19	650	39	[122]
2015	0.5 at.%	Graphene	2.2%	0.69	556	7.45	166.7	[40]
2016	0.5 at.%	Black Phosphorus	5%	0.157	363	3	175	[46]
Nd:Gd <sub>3</sub> Al <sub>x</sub> Ga <sub>5-x</sub> O <sub>12</sub> (Nd:GAGG)								
2010	0.74 at.%	V <sup>3+</sup> :YAG (T = 94%)	8%	0.29	18.2	2000	8	[115]
2011	0.74 at.%	Co <sup>2+</sup> :LMA (T = 90%)	8%	0.329	14.6	7100	3	[123]
Nd:(Lu <sub>x</sub> Gd <sub>1-x</sub> ) <sub>3</sub> Ga <sub>5</sub> O <sub>12</sub> (Nd:LGGG)								
2013	0.96 at.%	V <sup>3+</sup> :YAG (T = 95%)	8%	0.75	25.9	1700	17.1	[124]
2021	1 at.%	V <sup>3+</sup> :YAG (T = 90%)	5%	0.176	9.75	2400	8	[116]
Nd:Gd <sub>3x</sub> Y <sub>3(1-x)</sub> Sc <sub>2</sub> Ga <sub>3(1+δ)</sub> O <sub>12</sub> (Nd:GYSGG)								
2016	2 at.%	V <sup>3+</sup> :YAG (T = 90%)	8.8%	0.251	23.9	954	11	[29]
2017	1 at.%	Co:MgAl <sub>2</sub> O <sub>4</sub> (T = 82%)	12%	0.225	20.5	1319 *	9.1	[30]
Nd:Lu <sub>3</sub> Sc <sub>1.5</sub> Ga <sub>3.5</sub> O <sub>12</sub> (Nd:LuYSGG)								
			5%	0.39	-	-	41.6	[125]
2019	1 at.%	V <sup>3+</sup> :YAG (T = 90%)	10%	0.34	20.8	428	38.2	
2020	1 at.%	Bi <sub>2</sub> Se <sub>3</sub> (T = 75%)	5%	0.36	146	7.05	349.5	[49]

C<sub>Nd</sub>, Nd doping concentration; T<sub>OC</sub>, transmission of output coupler mirror; P<sub>Ave</sub>, average output power.

#### 2.4. The Other Types of Optical Crystals

In 1998, Demidovich et al. [20,126] demonstrated that LD-pumped Nd:KGd(WO<sub>4</sub>)<sub>2</sub> (Nd:KGW) can produce a continuous-wavelength laser output at 1.35  $\mu\text{m}$ . The stimulated emission cross section of Nd:KGW at 1351 nm is  $0.9 \times 10^{-19} \text{ cm}^2$ , and fluorescence lifetime is 98  $\mu\text{s}$ . In 2003, Savitski et al. [67] used V<sup>3+</sup>:YAG and PbS-doped glass as the SA and conducted comparative experiments. When the pump power was 47 mW, the output laser repetition rate reached 170 kHz, pulse width was 270 ns, and output power was 1 mW. With the V<sup>3+</sup>:YAG SA, the laser repetition rate was 100 kHz, pulse width was 250 ns, and output power was 5 mW. However, the output pulse width of this type of gain medium in the 1.3  $\mu\text{m}$  band was large and peak power was low.

Nd:YAP has a large emission cross section ( $1.8 \times 10^{-19} \text{ cm}^2$ ) at 1341 nm, long fluorescence lifetime (170  $\mu\text{s}$ ), and high thermal conductivity ( $11 \text{ W}\cdot\text{m}^{-1}\cdot\text{K}^{-1}$ ). It is an excellent solid-state laser gain medium. In 2015, Chen et al. [127] demonstrated a diode-side-pumped passively Q-switched Nd:YAP laser operating at 1.34  $\mu\text{m}$  with V<sup>3+</sup>:YAG SA. When the pump current was 34 A, the repetition rate of 5.51 kHz, pulse width of 197 ns, and maximum peak power of 6.93 kW were obtained. In 2016 Xu et al. [43] demonstrated a single and multi-wavelength Nd:YAP laser. The diode-pumped continuous-wave laser operated at 1364 nm by using a 0.08 mm glass etalon, and dual-wavelength laser was also achieved at 1328 and 1340 nm as well as at 1340 and 1364 nm. Replacing the etalons with Go SA, stable Q-switched laser operated at 1339 nm, the repetition rate of 76.9 kHz, pulse width of 380 ns, and maximum peak power of 14.5 W were obtained. The schematic of this laser is shown in Figure 7.

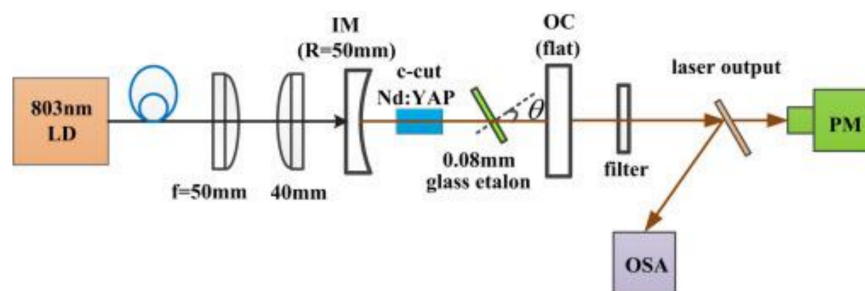


**Figure 7.** Set-up used for the LD-pumped Nd:YAP continuous-wave laser experiments. OSA, optical spectrum analyzer; PM, power meter; OC, output coupler [43].

Nd:LiYF<sub>4</sub> (Nd:YLF) is widely used, as it is suitable for lasers with different structures and pumping modes. Nd:YLF is a natural birefringence crystal, which has a long upper-level life ( $\sim 520 \mu\text{s}$ ) and small emission cross section ( $\sim 2\text{--}2.5 \times 10^{-20} \text{ cm}^2$ ; two polarizations). Hence, it possesses large energy storage capacity. In addition, owing to its high thermal conductivity ( $6 \text{ W}\cdot\text{m}^{-1}\cdot\text{K}^{-1}$ ) and negative thermal lens effect  $dn/dT$  ( $-4.3 \times 10^{-6} \pi$  polarization,  $-2 \times 10^{-6} \sigma$  polarization), it reduces the effect of the positive thermal lens. Moreover, it also has some advantages such as high crystal quality [128,129]. In 2013, Botha et al. [130] realized the Q-switched output of a Nd:YLF laser with maximum peak power of 6.1 kW at 1314 nm. In 2015, Xu et al. [48] reported a 1.3  $\mu\text{m}$  passively Q-switched Nd:YLF laser by using few-layer TI Bi<sub>2</sub>Se<sub>3</sub> as the SA. They obtained a pulse repetition rate of 161.3 kHz, shortest pulse width of 433 ns, and pulse energy of approximately 1.23  $\mu\text{J}$ .

Nd:LuLiF<sub>4</sub> (Nd:LLF) is an isostructure of Nd:YLF, which can also be used as a solid gain medium at the 1.3  $\mu\text{m}$  band. Compared with Nd:YLF, it has larger emission cross section ( $5.1 \times 10^{-20} \pi$  polarization,  $2.2 \times 10^{-20} \sigma$  polarization) and similar fluorescence lifetime (489  $\mu\text{s}$ ). In 2013, Li et al. [131] reported a dual-wavelength (1314 nm and 1321 nm) output of the Nd:LLF laser. When the repetition rate of the Q-switched pulse was 17.2 kHz, the peak power of 885 W was obtained. In 2019, Qian et al. [57] obtained a 227 kHz

high-repetition-rate pulse output by using gold nanorods (GNRs) with aspect ratio of 8 as the SA.

Several other types of optical crystals can also emit a 1.3  $\mu\text{m}$  laser, such as: Nd:Lu<sub>2</sub>O<sub>3</sub> [132,133] and Nd,Cr:YAG [33,134]. Here, we introduce only the main types. Table 5 presents the details of the research on the Nd:KGW, Nd:YAP, Nd:YLF, and Nd:LLF lasers.

**Table 5.** Research progress on 1.3  $\mu\text{m}$  passively Q-switched Nd:KGW, Nd:YAP, Nd:YLF, and Nd:LLF lasers.

Year	C <sub>Nd</sub>	SA	T <sub>OC</sub>	P <sub>Ave</sub> (W)	Pulse Width (ns)	Peak Power (W)	Repetition Rate (kHz)	Ref.
2001	4 at.%	V <sup>3+</sup> :YAG (T = 96.5%)	Nd:KGd(WO <sub>4</sub> ) <sub>2</sub> (Nd:KGW)	2%	0.087	40	27.6	[135]
2003	7 at.%	PbS (T = 97%)		4%	0.001	-	170	[67]
		V <sup>3+</sup> :YAG (T = 95%)			0.005	250	100	
		PbS (T = 98%)			0.012	50	31	
2006	3 at.%	V <sup>3+</sup> :YAG (T = 98%)		4%	0.042	7.6	58	[136]
2012	0.5 at.%	Graphene on SiC (T = 80%)	Nd:KLu(WO <sub>4</sub> ) <sub>2</sub> (Nd:KLW)	8%	0.89	-	135	[38]
			Nd:YAlO <sub>3</sub> (Nd:YAP)					
2006	Triangular Slab	V <sup>3+</sup> :YAG (T = 95.7%)		25%	-	77,000	-	[105]
2015	0.9 at.%	V <sup>3+</sup> :YAG (T = 93%)		7%	7.52	6930	5.51	[127]
2016	0.8 at.%	Graphene Oxide;		2.3%	0.43	14.7	76.9	[43]
			Nd:GdYAlO <sub>3</sub> (Nd:GYAP)					
2022	1 at.%	Bi nanosheets		5%	0.2	1.25	365	[137]
			Nd:LiYF <sub>4</sub> (Nd:YLF)					
2013	0.5 at.%	V <sup>3+</sup> :YAG (T = 97%)		5%	5.2	6100	6.3	[130]
2015	1 at.%	Bi <sub>2</sub> Se <sub>3</sub> (T = 95.1%)		2.3%	0.2	2.84	161.3	[48]
			Nd:LuLiF <sub>4</sub> (Nd:LLF)					
2013	1 at.%	V <sup>3+</sup> :YAG (T = 80%)		3%	1.87	885	17.2	[131]
				3.8%	1.03	84.9	91	
2016	1 at.%	Monolayer Graphene		8%	1.33	111.6	77	[42]
2017	1 at.%	g-C <sub>3</sub> N <sub>4</sub>		3.8%	0.96	275	154	[138]
		GNRs		3.8%	1.432	328	200	
		aspect ratio 5		8%	1.173	460	205	
2019	1 at.%	GNRs		3.8%	1.209	271	218	[57]
		aspect ratio 8		8%	1.247	438	227	

C<sub>Nd</sub>, Nd doping concentration; T<sub>OC</sub>, transmission of output coupler mirror; P<sub>Ave</sub>, average output power; g-C<sub>3</sub>N<sub>4</sub>, two-dimensional (2D) graphite carbon nitride; GNRs, gold nanorods.

### 3. Conclusions

#### 3.1. Summary

This review discussed 1.3  $\mu\text{m}$  laser crystals systematically. In recent years, the highest repetition rate of 1.3  $\mu\text{m}$  passively Q-switched laser has exceeded MHz, and highest peak power of 70 kW has been achieved. Although researchers have made great progress in 1.3  $\mu\text{m}$  passively Q-switched laser, there are also some factors limit the laser performance, such as, the low-gain emission line at 1.3  $\mu\text{m}$ , the heat accumulation of crystals, the stability at high repetition rate, and so on. We make a summary of 1.3  $\mu\text{m}$  passively Q-switched laser, and provide some research perspectives.

- The peak value of the gain medium at 1.06  $\mu\text{m}$  is much higher than that at 1.3  $\mu\text{m}$  in the fluorescence spectrum, and the transition probability at  $^4F_{3/2}$ - $^4I_{11/2}$  is greater than that at  $^4F_{3/2}$ - $^4I_{13/2}$ . Hence, it is necessary to suppress the 1.06  $\mu\text{m}$  wavelength oscillation in the cavity to obtain 1.3  $\mu\text{m}$  output light.
- When the stimulated emission cross section of the gain medium is large, the threshold can be reduced and laser oscillation can be easily realized, whereas a small stimulated emission cross section of the gain medium can improve the energy storage capacity. Long fluorescence lifetime can increase the accumulation of upper-level particles and obtain larger energy storage, whereas short fluorescence lifetime is beneficial in obtaining a stable high-repetition-rate pulse output. Therefore, further in-depth research is required on the gain medium materials.
- Owing to the differences in the band gap, nonlinear absorption, and saturated absorption of the SA materials, the ground-state absorption cross section, excited-state absorption loss, modulation depth, and damage threshold are different.
- The resonator design (flat–flat, plane–concave, Z-cavity, V-cavity) affects the laser performance. The flat–flat cavity has the advantages of good directivity and large

mode volume, and it is easy to obtain single-mode oscillations with this cavity. The Z-shaped cavity can not only adjust the focusing position and mode matching, but also limit the output beam astigmatism with a smaller folding angle. V-cavity can adjust the mode matching of the pump light, prevent the SA from absorbing the residual pump energy. The plane–concave cavity can improve the effective area ratio between of the gain medium and the SA, and achieves a compact structure while meeting the second threshold condition.

- The pump source’s power, center wavelength and mode matching influence the output power.
- Pulse fluctuations of the passively Q-switched laser, caused by the thermal lens effect also influence the output power.

### 3.2. Outlook

In view of the existing problems, researchers have put forward the following solutions from different perspectives. These improvement measures effectively accelerate and promote the development of 1.3  $\mu\text{m}$  passively Q-switched laser. So, they also represent the current research trend.

- New crystals of better quality: researchers have continuously developed new crystals, such as Nd:GYSGG, Nd: (Lu Gd Y La)  $\text{VO}_4$  mixed crystals, and Nd,Cr:YAG, etc. These crystals not only improve the performance, but can also be applied to some special fields due to their unique properties.
- $\text{V}^{3+}$ :YAG and Co:LMA are popular 1.3  $\mu\text{m}$  wavelength Q-switched devices. They have great absorption of the 1.3  $\mu\text{m}$  wavelength and can be easily bleached. Hence, they achieve good experimental results (pulse width of several ns, peak power approaching the order of MW). During the past few decades, many new SA materials have been used as Q-switch devices such as graphene, black phosphorus, gold nanomaterials, and MXene. These materials can obtain high-repetition-rate pulse output (several hundreds of kHz), but their peak power is very low (few tens of W).
- Optimization of resonant cavity: selecting the appropriate cavity type and device can reduce the unsaturated absorption loss in the cavity, thereby improving the output light quality. For example, the combination of SA and coupling output mirror transmittance can affect the repetition frequency, pulse width, and power of the output pulses. The laser output power can be improved through lamp pumping, multi-LD side pumping, slab gain medium, and multi-wavelength output. The pulse width can be compressed by using double SA, composite crystal, and mode-locking.
- Reducing the thermal effect: the thermal effect of high-thermal-conductivity crystals and composite crystals can be reduced by using a thermoelectric cooler for controlling the crystal temperature.
- Reducing timing and amplitude jitter: researchers have proposed various methods to reduce the pulse jitter, such as external modulation, pulsed LD pump source, self-injection seeding, and pre-pumping mechanism.

**Author Contributions:** Conceptualization, X.F. (Xihong Fu) and X.F. (Xinpeng Fu); methodology, X.F. (Xihong Fu) and X.F. (Xinpeng Fu); investigation, Y.S.; resources, X.F. (Xihong Fu) and Y.N.; data curation, Y.S.; writing—original draft preparation, Y.S.; writing—review and editing, Y.S., X.F. (Xihong Fu) and X.F. (Xinpeng Fu); visualization, C.Y., W.L. and X.Z.; supervision, X.F. (Xihong Fu) and X.F. (Xinpeng Fu); project administration, X.F. (Xihong Fu) and Y.N.; funding acquisition, X.F. (Xihong Fu) and Y.W. All authors have read and agreed to the published version of the manuscript.

**Funding:** This research was funded by Science and Technology Development Project of Jilin Province (grant numbers 20200401060GX, 20210201028GX, 20200501008GX).

**Institutional Review Board Statement:** Not applicable.

**Informed Consent Statement:** Not applicable.

**Data Availability Statement:** Not applicable.

**Conflicts of Interest:** The authors declare no conflict of interest.

## References

1. Zheng, Y.H.; Wu, Z.Q.; Huo, M.R.; Zhou, H.J. Generation of a continuous-wave squeezed vacuum state at 1.3  $\mu\text{m}$  by employing a home-made all-solid-state laser as pump source. *Chin. Phys.* **2013**, *22*, 431–434. [[CrossRef](#)]
2. Zhu, W.; Liu, Q.; Wu, Y. Aerosol absorption measurement at SWIR with water vapor interference using a differential photoacoustic spectrometer. *Opt. Express* **2015**, *23*, 23108–23116. [[CrossRef](#)]
3. Sorokin, E.; Naumov, S.; Sorokina, I.T. Ultrabroadband infrared solid-state lasers. *IEEE J. Sel. Top. Quantum Electron.* **2005**, *11*, 690–712. [[CrossRef](#)]
4. Zhou, H.Q.; Bi, X.L.; Zhu, S.Q.; Li, Z.; Yin, H.; Zhang, P.X.; Chen, Z.Q.; Lv, Q.T. Multi-wavelength passively Q-switched red lasers with  $\text{Nd}^{3+}$ :YAG/YAG/ $\text{V}^{3+}$ :YAG/YAG composite crystal. *Opt. Quantum Electron.* **2018**, *50*, 56. [[CrossRef](#)]
5. Tu, W.; Shang, L.Q.; Dai, S.B.; Zong, N.; Wang, Z.M.; Zhang, F.F.; Chen, Y.; Liu, K.; Zhang, S.J.; Yang, F.; et al. 0.95 W high-repetition-rate, picosecond 335 nm laser based on a frequency quadrupled, diode-pumped Nd:YVO<sub>4</sub> MOPA system. *Appl. Opt.* **2015**, *54*, 6182–6185. [[CrossRef](#)]
6. Li, Y.L.; Yao, J.B.; Zeng, Y.H.; Zhang, Y.L. Sum-frequency yellow light laser. *J. Changchun Univ. Sci. Technol. (Nat. Sci. Ed.)* **2010**, *33*, 51–53.
7. Niu, X. Extracavity all-solid-state eye-safe Raman laser based on Ba(NO<sub>3</sub>)<sub>2</sub> crystal pumped by 1342nm laser. Master's Thesis, Beijing University of Technology, Beijing, China, 2016.
8. Zhang, D.; Su, L.; Li, H.; Qian, X.; Xu, J. Characteristics and optical spectra of V:YAG crystal grown in reducing atmosphere. *J. Cryst. Growth* **2006**, *294*, 437–441. [[CrossRef](#)]
9. Ge, W.; Zhang, H.; Wang, J.; Ran, D.; Sun, S.; Xia, H.; Liu, J.; Xu, X.; Hu, X.; Jiang, M. Growth and thermal properties of  $\text{Co}^{2+}$ :LaMgAl<sub>11</sub>O<sub>19</sub> crystal. *J. Cryst. Growth* **2005**, *282*, 320–329. [[CrossRef](#)]
10. Zhang, G.; Wang, Y.; Wang, J.; Jiao, Z. Passively Q-switched laser at 1.34  $\mu\text{m}$  using a molybdenum disulfide saturable absorber. *Infrared Phys. Technol.* **2019**, *96*, 311–315. [[CrossRef](#)]
11. Chu, Z.; Zhang, H.; Wu, Y.; Zhang, C.; Liu, J.; Yang, J. Passively Q-switched laser based on gold nanobipyramids as saturable absorbers in the 1.3  $\mu\text{m}$  region. *Opt. Commun.* **2018**, *406*, 209–213. [[CrossRef](#)]
12. Zhang, G.; Tu, H.; Liu, Y.; Hu, Z. Heat treatment and optical absorption studies on Nd:YVO<sub>4</sub> crystal. *J. Cryst. Growth* **2009**, *311*, 912–915. [[CrossRef](#)]
13. Saeedi, H.; Yadegari, M.; Enayati, S.; Asadian, M.; Shojaei, M.; Khodaei, Y.; Mirzaei, N.; Mashayekhi Asl, I. Thermal shocks influence on the growth process and optical quality of Nd: YAG crystal. *J. Cryst. Growth* **2013**, *363*, 171–175. [[CrossRef](#)]
14. Asadian, M.; Hajiesmaeilbaigi, F.; Mirzaei, N.; Saeedi, H.; Khodaei, Y.; Enayati, S. Composition and dissociation processes analysis in crystal growth of Nd:GGG by the Czochralski method. *J. Cryst. Growth* **2010**, *312*, 1645–1650. [[CrossRef](#)]
15. Senthil Kumaran, A.; Moorthy Babu, S.; Ganesamoorthy, S.; Bhaumik, I.; Karnal, A.K. Crystal growth and characterization of KY(WO<sub>4</sub>)<sub>2</sub> and KGd(WO<sub>4</sub>)<sub>2</sub> for laser applications. *J. Cryst. Growth* **2006**, *292*, 368–372. [[CrossRef](#)]
16. Bowkett, G.C.; Baxter, G.W.; Booth, D.J.; Taira, T.; Teranishi, H.; Kobayashi, T. Single-mode 1.34- $\mu\text{m}$  Nd:YVO<sub>4</sub> microchip laser with cw Ti:sapphire and diode-laser pumping. *Opt. Lett.* **1994**, *19*, 957–959. [[CrossRef](#)]
17. Zagumennyi, A.I.; Ostroumov, V.G.; Shcherbakov, I.A.; Jensen, T.; Meyen, J.P.; Huber, G. The Nd:GdVO<sub>4</sub> crystal: A new material for diode-pumped lasers. *Sov. J. Quantum Electron.* **1992**, *22*, 1071. [[CrossRef](#)]
18. Geusic, J.E.; Marcos, H.M.; Van Uitert, L. Laser oscillations in Nd-doped yttrium aluminum, yttrium gallium and gadolinium garnets. *Appl. Phys. Lett.* **1964**, *4*, 182–184. [[CrossRef](#)]
19. Yoshida, K.; Yoshida, H.; Kato, Y. Characterization of high average power Nd:GGG slab lasers. *IEEE J. Quantum Electron.* **1988**, *24*, 1188–1192. [[CrossRef](#)]
20. Demidovich, A.A.; Kuzmin, A.N.; Ryabtsev, G.I.; Strek, W.; Titov, A.N. A 1.35  $\mu\text{m}$  laser diode pumped continuous wave KGW:Nd laser. *Spectrochim. Acta Part A Mol. Biomol. Spectrosc.* **1998**, *54*, 1711–1713. [[CrossRef](#)]
21. Helena, J.; Pavel, C.; Jan, S.; Jan Karol, J.; Krzysztof, K.; Waldemar, Z.; Zygmunt, M.; Mitsunobu, M. In Passively mode-locked Q-switched Nd:YAP 1.34- $\mu\text{m}$ /1.08- $\mu\text{m}$  laser with efficient hollow-waveguide radiation delivery. In *Solid State Lasers XI: High-Power Lasers and Applications*; SPIE: San Jose, CA, USA, 2002.
22. Nikkinen, J.; Korpijärvi, V.M.; Leino, I.; Härkönen, A.; Guina, M. Microchip laser Q-switched with GaInNAs/GaAs SESAM emitting 204 ps pulses at 1342 nm. *Electron. Lett.* **2015**, *51*, 850–852. [[CrossRef](#)]
23. Wang, Z.; Zhang, B.; Ning, J.; Zhang, X.; Su, X.; Zhao, R. High-peak-power passively Q-switched 1.3  $\mu\text{m}$  Nd:YAG/ $\text{V}^{3+}$ :YAG laser pumped by a pulsed laser diode. *Chin. Opt. Lett.* **2015**, *13*, 021403–21406. [[CrossRef](#)]
24. Dong, L.; Li, D.; Pan, H.; Li, Y.; Zhao, S.; Li, G.; Chu, H. Pulse characteristics from a MoSe<sub>2</sub> Q-switched Nd:GdVO<sub>4</sub> laser at 1.3  $\mu\text{m}$ . *Appl. Opt.* **2019**, *58*, 8194–8199. [[CrossRef](#)]
25. Li, X. Research on 1.3  $\mu\text{m}$  short pulse laser characteristics of LD-pumped Nd-doped vanadate crystals. Ph.D. Thesis, Shan Dong University, Jinan, China, April 2012.
26. Wang, S.; Li, Q.; Du, S.; Zhang, Q.; Shi, Y.; Xing, J.; Zhang, D.; Feng, B.; Zhang, Z.; Zhang, S. Self-Q-switched and mode-locked Nd,Cr:YAG laser with 6.52-W average output power. *Opt. Commun.* **2007**, *277*, 130–133. [[CrossRef](#)]
27. Li, J.; Wu, Y.S.; Pan, Y.B.; Zhu, Y.; Guo, J.K. Spectral properties of Nd,Cr:YAG self-Q-switched laser transparent ceramics. *Chin. J. Lumin.* **2007**, 219–224.

28. Zhong, K.; Sun, C.L.; Yao, J.Q.; Xu, D.G.; Pei, Y.Q.; Zhang, Q.L.; Luo, J.Q.; Sun, D.L.; Yin, S.T. Continuous-wave Nd:GYSGG laser around 1.3  $\mu\text{m}$ . *Laser Phys. Lett.* **2012**, *9*, 491–495. [[CrossRef](#)]
29. Song, T.; Li, P.; Chen, X.; Ma, B.; Dun, Y. Passively Q-switched Nd:GYSGG laser operating at 1.3  $\mu\text{m}$  with V:YAG as saturable absorber. *Optik* **2016**, *127*, 10621–10625. [[CrossRef](#)]
30. Lin, H.-Y.; Sun, D.; Copner, N.; Zhu, W.-Z. Nd:GYSGG laser at 1331.6 nm passively Q-switched by a Co:MgAl<sub>2</sub>O<sub>4</sub> crystal. *Opt. Mater.* **2017**, *69*, 250–253. [[CrossRef](#)]
31. Huang, H.-T.; Zhang, B.-T.; He, J.-L.; Yang, J.-F.; Xu, J.-L.; Yang, X.-Q.; Zuo, C.-H.; Zhao, S. Diode-pumped passively Q-switched Nd:Gd<sub>0.5</sub>Y<sub>0.5</sub>VO<sub>4</sub> laser at 1.34  $\mu\text{m}$  with V<sup>3+</sup>:YAG as the saturable absorber. *Opt. Express* **2009**, *17*, 6946–6951. [[CrossRef](#)]
32. Li, X.; Li, G.Q.; Zhao, S.Z.; Zhao, B.; Li, Y.F.; Yin, L. CW and passively Q-switched laser performance of a mixed c-cut Nd:Gd<sub>0.33</sub>Lu<sub>0.33</sub>Y<sub>0.33</sub>VO<sub>4</sub> crystal operating at 1.34  $\mu\text{m}$ . *Opt. Mater.* **2011**, *34*, 159–163. [[CrossRef](#)]
33. Lin, B.; Zhang, Q.-L.; Zhang, D.-X.; Feng, B.-H.; He, J.-L.; Zhang, J.-Y. Passively Q-Switched Nd,Cr:YAG Laser Simultaneous Dual-Wavelength Operation at 946 nm and 1.3  $\mu\text{m}$ . *Chin. Phys. Lett.* **2016**, *33*, 074203. [[CrossRef](#)]
34. Ma, J.S.; Li, Y.F.; Sun, Y.M.; Qi, H.J.; Lan, R.J.; Hou, X.Y. Passively Q-switched 1.34  $\mu\text{m}$  Nd:GdVO<sub>4</sub> laser with V:YAG saturable absorber. *Laser Phys. Lett.* **2008**, *5*, 593. [[CrossRef](#)]
35. Kane, T.J.; Clarkson, W.A.; Shori, R.K. 1.34  $\mu\text{m}$  Nd:YVO<sub>4</sub> laser passively Q-switched by V:YAG and optimized for lidar. In *Solid State Lasers XXIX: Technology and Devices*; SPIE: San Francisco, CA, USA, 2020; Volume 11259.
36. Yang, F.; Li, M.; Zhao, S.; Fu, X.H.; Gao, L.L. Research progress on passively Q-switched lasers based on new saturable absorption devices. *Laser Optoelectron. Prog.* **2020**, *57*, 15.
37. Liang, L.; Lin, Z.H.; Chen, S.; Wang, J.X. Graphene passively Q-switching for dual-wavelength lasers at 1064 nm and 1342 nm in Nd:YVO<sub>4</sub> laser. *Chin. J. Laser* **2014**, *41*, 53–56. [[CrossRef](#)]
38. Shen, H.; Wang, Q.; Zhang, X.; Liu, Z.; Bai, F.; Cong, Z.; Chen, X.; Gao, L.; Zhang, H.; Xu, X.; et al. Passively-switched Nd:KLu(WO<sub>4</sub>)<sub>2</sub> laser at 1355 nm with graphene on SiC as saturable absorber. *Appl. Phys. Express* **2012**, *5*, 092703. [[CrossRef](#)]
39. Zhang, L.; Yu, H.; Yan, S.; Zhao, W.; Sun, W.; Yang, Y.; Wang, L.; Hou, W.; Lin, X.; Wang, Y.; et al. A 1319 nm diode-side-pumped Nd:YAG laser Q-switched with graphene oxide. *J. Mod. Opt.* **2013**, *60*, 1287–1289. [[CrossRef](#)]
40. Xu, B.; Wang, Y.; Cheng, Y.; Yang, H.; Xu, H.; Cai, Z. Nanosecond pulse generation in a passively Q-switched Nd:GGG laser at 1331 nm by CVD graphene saturable absorber. *J. Opt.* **2015**, *17*, 105501. [[CrossRef](#)]
41. Feng, C.; Zhang, H.; Wang, Q.; Xu, S.; Fang, J. 1357 nm passively Q-switched crystalline ceramic laser based on multilayer graphene. *Laser Phys.* **2016**, *26*, 055802. [[CrossRef](#)]
42. Li, S.; Li, T.; Zhao, S.; Li, G.; Hang, Y.; Zhang, P. 1.31 and 1.32  $\mu\text{m}$  dual-wavelength Nd:LuLiF<sub>4</sub> laser. *Opt. Laser Technol.* **2016**, *81*, 14–17.
43. Xu, B.; Wang, Y.; Lin, Z.; Peng, J.; Cheng, Y.; Luo, Z.; Xu, H.; Cai, Z.; Weng, J.; Moncorgé, R. Single- and multi-wavelength Nd:YAlO<sub>3</sub> lasers at 1328, 1339 and 1364 nm. *Opt. Laser Technol.* **2016**, *81*, 1–6. [[CrossRef](#)]
44. Lin, H.Y.; Zhao, M.J.; Lin, H.J.; Wang, Y.P. Graphene-oxide as saturable absorber for a 1342 nm Q-switched Nd:YVO<sub>4</sub> laser. *Optik* **2017**, *135*, 129–133. [[CrossRef](#)]
45. Zhang, H.; Peng, J.; Yang, X.; Ma, C.; Zhao, Q.; Chen, G.; Su, X.; Li, D.; Zheng, Y. Passively Q-switched Nd:YVO<sub>4</sub> laser operating at 1.3  $\mu\text{m}$  with a graphene oxide and ferroferric-oxide nanoparticle hybrid as a saturable absorber. *Appl. Opt.* **2020**, *59*, 1741–1745. [[CrossRef](#)]
46. Han, S.; Zhang, F.; Wang, M.; Wang, L.; Zhou, Y.; Wang, Z.; Xu, X. Black phosphorus based saturable absorber for Nd-ion doped pulsed solid state laser operation. *Indian J. Phys.* **2016**, *91*, 439–443. [[CrossRef](#)]
47. Sun, X.; Nie, H.; He, J.; Zhao, R.; Su, X.; Wang, Y.; Zhang, B.; Wang, R.; Yang, K. Passively Q-Switched Nd:GdVO<sub>4</sub> 1.3  $\mu\text{m}$  laser with few-layered black phosphorus saturable absorber. *IEEE J. Sel. Top. Quantum Electron.* **2018**, *24*, 1600405. [[CrossRef](#)]
48. Xu, B.; Wang, Y.; Peng, J.; Luo, Z.; Xu, H.; Cai, Z.; Weng, J. Topological insulator Bi<sub>2</sub>Se<sub>3</sub> based Q-switched Nd:LiYF<sub>4</sub> nanosecond laser at 1313 nm. *Opt Express* **2015**, *23*, 7674–7680. [[CrossRef](#)]
49. Wang, B. Passively-Q-switched 1.33  $\mu\text{m}$  Nd:LuYSGG laser with the Bi<sub>2</sub>Se<sub>3</sub> topological insulator as a saturable absorber. *J. Russ. Laser Res.* **2020**, *41*, 358–363. [[CrossRef](#)]
50. Wang, K.; Yang, K.; Zhang, X.; Zhao, S.; Luan, C.; Liu, C.; Wang, J.; Xu, X.; Xu, J. Passively Q-switched laser at 1.3  $\mu\text{m}$  with few-layered MoS<sub>2</sub> saturable absorber. *IEEE J. Sel. Top. Quantum Electron.* **2017**, *23*, 71–75. [[CrossRef](#)]
51. Yan, B.; Zhang, B.; Nie, H.; Li, G.; Sun, X.; Wang, Y.; Liu, J.; Shi, B.; Liu, S.; He, J. Broadband 1T-titanium selenide-based saturable absorbers for solid-state bulk lasers. *Nanoscale* **2018**, *10*, 20171–20177. [[CrossRef](#)]
52. Lin, M.; Peng, Q.; Hou, W.; Fan, X.; Liu, J. 1.3  $\mu\text{m}$  Q-switched solid-state laser based on few-layer ReS<sub>2</sub> saturable absorber. *Opt. Laser Technol.* **2019**, *109*, 90–93. [[CrossRef](#)]
53. Liu, S.; Wang, M.; Yin, S.; Xie, Z.; Wang, Z.; Zhou, S.; Chen, P. Nonlinear optical properties of few-layer rhenium disulfide nanosheets and their passively Q-switched laser application. *Phys. Status Solidi (A)* **2019**, *216*, 1800837. [[CrossRef](#)]
54. Wang, M.; Wang, Z.; Xu, X.; Duan, S.; Du, C. Tin diselenide-based saturable absorbers for eye-safe pulse lasers. *Nanotechnology* **2019**, *30*, 265703. [[CrossRef](#)]
55. Zhang, G.; Wang, Y.; Jiao, Z.; Li, D.; Wang, J.; Chen, Z. Tungsten disulfide saturable absorber for passively Q-Switched YVO<sub>4</sub>/Nd:YVO<sub>4</sub>/YVO<sub>4</sub> laser at 1342.2 nm. *Opt. Mater.* **2019**, *92*, 95–99. [[CrossRef](#)]
56. Yang, Z.; Han, L.; Zhang, J.; Zhang, Y.; Zhang, F.; Lin, Z.; Ren, X.; Yang, Q.; Zhang, H. Passively Q-switched laser using PtSe<sub>2</sub> as saturable absorber at 1.3  $\mu\text{m}$ . *Infrared Phys. Technol.* **2020**, *104*, 103155. [[CrossRef](#)]

57. Qian, Q.; Wang, N.; Zhao, S.; Li, G.; Li, T.; Li, D.; Yang, K.; Zang, J.; Ma, H. Gold nanorods as saturable absorbers for the passively Q-switched Nd:LLF laser at 1.34  $\mu\text{m}$ . *Chin. Opt. Lett.* **2019**, *17*, 041401. [[CrossRef](#)]
58. Wang, C.; Peng, Q.-Q.; Fan, X.-W.; Liang, W.-Y.; Zhang, F.; Liu, J.; Zhang, H. MXene  $\text{Ti}_3\text{C}_2\text{T}_x$  saturable absorber for pulsed laser at 1.3  $\mu\text{m}$ . *Chin. Phys. B* **2018**, *27*, 094214. [[CrossRef](#)]
59. Wang, J.; Liu, S.; Wang, Y.; Wang, T.; Shang, S.; Ren, W. Magnetron-sputtering deposited molybdenum carbide MXene thin films as a saturable absorber for passively Q-switched lasers. *J. Mater. Chem. C* **2020**, *8*, 1608–1613. [[CrossRef](#)]
60. Wang, J.; Wang, Y.; Liu, S.; Li, G.; Zhang, G.; Cheng, G. Nonlinear Optical Response of Reflective MXene Molybdenum Carbide Films as Saturable Absorbers. *Nanomaterials (Basel)* **2020**, *10*. [[CrossRef](#)]
61. O'Connor, J.R. Unusual crystal-field energy levels and efficient laser properties of  $\text{YVO}_4:\text{Nd}$ . *Appl. Phys. Lett.* **1966**, *9*, 407–409. [[CrossRef](#)]
62. Xue, Q.H.; Zheng, Q.; Bu, Y.K.; Qian, L.S. LD-pumped Nd:YVO<sub>4</sub>/V:YAG passively Q-switched 1.34  $\mu\text{m}$  laser. *Acta Photonica Sinica* **2005**, *34*, 971–974.
63. Tucker, A.W.; Birnbaum, M.; Fincher, C.L.; DeShazer, L.G. Continuous-wave operation of Nd:YVO<sub>4</sub> at 1.06 and 1.34  $\mu\text{m}$ . *J. Appl. Phys.* **1976**, *47*, 232–234. [[CrossRef](#)]
64. Fluck, R.; Braun, B.; Gini, E.; Melchior, H.; Keller, U. Passively Q-switched 1.34- $\mu\text{m}$  Nd:YVO<sub>4</sub> microchip laser with semiconductor saturable-absorber mirrors. *Opt. Lett.* **1997**, *22*, 991–993. [[CrossRef](#)]
65. Lai, H.C.; Li, A.; Su, K.W.; Ku, M.L.; Chen, Y.F.; Huang, K.F. InAs/GaAs quantum-dot saturable absorbers for diode-pumped passively Q-switched Nd-doped 1.3- $\mu\text{m}$  lasers. *Opt. Lett.* **2005**, *30*, 480–482. [[CrossRef](#)]
66. Janousek, J.; Tidemand-Lichtenberg, P.; Mortensen, J.L.; Buchhave, P. Investigation of passively synchronized dual-wavelength Q-switched lasers based on V:YAG saturable absorber. *Opt. Commun.* **2006**, *265*, 277–282. [[CrossRef](#)]
67. Savitski, V.G.; Malyarevich, A.M.; Yumashev, K.V.; Sinclair, B.D.; Lipovskii, A.A. Diode-pumped Nd:YVO<sub>4</sub> and Nd:KGd(WO<sub>4</sub>)<sub>2</sub> 1.3  $\mu\text{m}$  lasers passively Q-switched with PbS-doped glass. *Appl. Phys. B* **2003**, *76*, 253–256. [[CrossRef](#)]
68. Li, A.; Liu, S.C.; Su, K.W.; Liao, Y.L.; Huang, S.C.; Chen, Y.F.; Huang, K.F. InGaAsP quantum-wells saturable absorber for diode-pumped passively Q-switched 1.3- $\mu\text{m}$  lasers. *Appl. Phys. B* **2006**, *84*, 429–431. [[CrossRef](#)]
69. Huang, H.T.; He, J.L.; Zuo, C.H.; Zhang, H.J.; Wang, J.Y.; Liu, Y.; Wang, H.T. Co<sup>2+</sup>: LMA crystal as saturable absorber for a diode-pumped passively Q-switched Nd:YVO<sub>4</sub> laser at 1342 nm. *Appl. Phys. B* **2007**, *89*, 319–321. [[CrossRef](#)]
70. Xu, J.L.; Huang, H.T.; He, J.L.; Yang, J.F.; Zhang, B.T.; Yang, X.Q.; Liu, F.Q. Dual-wavelength oscillation at 1064 and 1342 nm in a passively Q-switched Nd:YVO<sub>4</sub> laser with V<sup>3+</sup>:YAG as saturable absorber. *Appl. Phys. B* **2011**, *103*, 75–82. [[CrossRef](#)]
71. Zhai, Y.; Wang, J.X.; Wang, Y.F. Optical characteristic of nc-Si/SiN<sub>x</sub> film and its Q-Switching to 1342 nm laser. *Laser J.* **2011**, *32*, 10–11.
72. Wang, M.; Zhang, F.; Wang, Z.; Wu, Z.; Xu, X. Passively Q-switched Nd<sup>3+</sup> solid-state lasers with antimonene as saturable absorber. *Opt. Express* **2018**, *26*, 4085–4095. [[CrossRef](#)]
73. Pan, H.; Chu, H.; Li, Y.; Li, G.; Zhao, S.; Li, D. Bismuth functionalized GaAs as saturable absorber for passive Q-switching at 1.34  $\mu\text{m}$ . *Opt. Mater.* **2019**, *98*, 109457. [[CrossRef](#)]
74. Zhang, H.; Peng, J.; Yao, J.; Yang, X.; Li, D.; Zheng, Y. 1.3  $\mu\text{m}$  passively Q-switched mode-locked laser with Fe<sub>3</sub>O<sub>4</sub> nanoparticle saturable absorber. *Laser Phys.* **2020**, *30*, 125801. [[CrossRef](#)]
75. Zhang, T.; Wang, M.; Xue, Y.; Xu, J.; Xie, Z.; Zhu, S. Liquid metal as a broadband saturable absorber for passively Q-switched lasers. *Chin. Opt. Lett.* **2020**, *18*, 111901. [[CrossRef](#)]
76. Cao, L.; Chu, H.; Pan, H.; Wang, R.; Li, Y.; Zhao, S.; Li, D.; Zhang, H.; Li, D. Nonlinear optical absorption features in few-layered hybrid  $\text{Ti}_3\text{C}_2(\text{OH})_2/\text{Ti}_3\text{C}_2\text{F}_2$  MXene for optical pulse generation in the NIR region. *Opt. Express* **2020**, *28*, 31499–31509. [[CrossRef](#)]
77. Zhang, T.; Chu, H.; Li, Y.; Zhao, S.; Ma, X.; Pan, H.; Li, D. Third-order optical nonlinearity in Ti<sub>2</sub>C MXene for Q-switching operation at 1–2  $\mu\text{m}$ . *Opt. Mater.* **2022**, *124*, 112054. [[CrossRef](#)]
78. Zhang, H.; Meng, X.; Liu, J.; Zhu, L.; Wang, C.; Shao, Z.; Wang, J.; Liu, Y. Growth of lowly Nd doped GdVO<sub>4</sub> single crystal and its laser properties. *J. Cryst. Growth* **2000**, *216*, 367–371. [[CrossRef](#)]
79. Qi, H.J.; Liu, X.D.; Hou, X.Y.; Li, Y.F.; Sun, Y.M. A c-cut Nd:GdVO<sub>4</sub> solid-state laser passively Q-switched with Co<sup>2+</sup>:LaMgAl<sub>11</sub>O<sub>19</sub> lasing at 1.34  $\mu\text{m}$ . *Laser Phys. Lett.* **2007**, *4*, 576–579. [[CrossRef](#)]
80. Li, Y.F.; Zhao, S.Z.; Sun, Y.M.; Qi, H.J.; Cheng, K. Diode-pumped doubly passively Q-switched c-cut Nd:GdVO<sub>4</sub> 1.34  $\mu\text{m}$  laser with V<sup>3+</sup>:YAG and Co:LMA saturable absorbers. *Opt. Laser Technol.* **2011**, *43*, 985–988. [[CrossRef](#)]
81. Ma, J.; Li, Y.; Sun, Y.; Xu, J.; He, J. Diode-pumped passively Q-switched Nd:GdVO<sub>4</sub> laser at 1342 nm with V:YAG saturable absorber. *Opt. Commun.* **2009**, *282*, 958–961. [[CrossRef](#)]
82. Xu, C.; Li, G.; Zhao, S.; Li, X.; Cheng, K.; Zhang, G.; Li, T. LD-pumped passively Q-switched Nd:GdVO<sub>4</sub> laser at 1342 nm with high initial transmission V:YAG saturable absorber. *Laser Phys.* **2010**, *20*, 1335–1340. [[CrossRef](#)]
83. Pan, H.; Wang, X.; Chu, H.; Li, Y.; Zhao, S.; Li, G.; Li, D. Optical modulation characteristics of zeolitic imidazolate framework-67 (ZIF-67) in the near infrared regime. *Opt. Lett.* **2019**, *44*, 5892–5895. [[CrossRef](#)]
84. Su, X.; Wang, Y.; Zhang, B.; Zhang, H.; Yang, K.; Wang, R.; He, J. Bismuth quantum dots as an optical saturable absorber for a 1.3  $\mu\text{m}$  Q-switched solid-state laser. *Appl. Opt.* **2019**, *58*, 1621–1625. [[CrossRef](#)]
85. Dong, L.; Huang, W.; Chu, H.; Li, Y.; Wang, Y.; Zhao, S.; Li, G.; Zhang, H.; Li, D. Passively Q-switched near-infrared lasers with bismuthene quantum dots as the saturable absorber. *Opt. Laser Technol.* **2020**, *128*, 106219. [[CrossRef](#)]

86. Feng, X.; Liu, J.; Yang, W.; Yu, X.; Jiang, S.; Ning, T.; Liu, J. Broadband indium tin oxide nanowire arrays as saturable absorbers for solid-state lasers. *Opt. Express* **2020**, *28*, 1554–1560. [[CrossRef](#)]
87. Zhang, J.; Wang, Y.; Mu, W.; Jia, Z.; Zhang, B.; He, J.; Tao, X. New near-infrared optical modulator of  $\text{Co}^{2+}:\beta\text{-Ga}_2\text{O}_3$  single crystal. *Opt. Mater. Express* **2021**, *11*. [[CrossRef](#)]
88. Dong, L.; Chu, H.; Li, Y.; Zhao, S.; Li, G.; Li, D. Nonlinear optical responses of  $\alpha\text{-Fe}_2\text{O}_3$  nanosheets and application as a saturable absorber in the wide near-infrared region. *Opt. Laser Technol.* **2021**, *136*, 106812.
89. Zhang, C.; Zheng, L.; Chu, H.; Pan, H.; Hu, Y.; Li, D.; Dong, L.; Zhao, S.; Li, D. Monoclinic bismuth vanadate nanoparticles as saturable absorber for Q-switching operations at 1.3 and 2  $\mu\text{m}$ . *Appl. Phys. Express* **2022**, *15*, 072004. [[CrossRef](#)]
90. Maunier, C.; Doualan, J.L.; Moncorgé, R.; Speghini, A.; Bettinelli, M.; Cavalli, E. Growth, spectroscopic characterization, and laser performance of Nd:LuVO<sub>4</sub> a new infrared laser material that is suitable for diode pumping. *J. Opt. Soc. Am. B* **2002**, *19*, 1794–1800. [[CrossRef](#)]
91. Zhang, H.; Liu, J.; Wang, J.; Xu, X.; Jiang, M. Continuous-wave laser performance of Nd:LuVO<sub>4</sub> crystal operating at 1.34  $\mu\text{m}$ . *Appl. Opt.* **2005**, *44*, 7439–7441. [[CrossRef](#)]
92. Ran, D.; Xia, H.; Sun, S.; Liu, F.; Ling, Z.; Ge, W.; Zhang, H.; Wang, J. Thermal properties of a Nd:LuVO<sub>4</sub> crystal. *Cryst. Res. Technol.* **2007**, *42*, 920–925. [[CrossRef](#)]
93. Liu, F.; He, J.; Zhang, B.; Xu, J.; Dong, X.; Yang, K.; Xia, H.; Zhang, H. Diode-pumped passively Q-switched Nd:LuVO<sub>4</sub> laser at 1.34  $\mu\text{m}$  with a  $\text{V}^{3+}$ :YAG saturable absorber. *Opt. Express* **2008**, *16*, 11759–11763. [[CrossRef](#)]
94. Liu, F.Q.; He, J.L.; Xu, J.L.; Yang, J.F.; Zhang, B.T.; Huang, H.T.; Gao, C.Y.; Xu, J.Q.; Zhang, H.J. Passive Q-switching performance with Co:LMA crystal in a diode-pumped Nd:LuVO<sub>4</sub> laser. *Laser Phys.* **2010**, *20*, 786–789. [[CrossRef](#)]
95. Yu, Y.; Wang, J.; Zhang, H.; Yu, H.; Wang, Z.; Jiang, M.; Xia, H.; Boughton, R.I. Growth and characterization of Nd:Y<sub>x</sub>Gd<sub>1-x</sub>VO<sub>4</sub> series laser crystals. *J. Opt. Soc. Am. B* **2008**, *25*, 995–1001. [[CrossRef](#)]
96. Li, P.; Li, Y.; Sun, Y.; Hou, X.; Zhang, H.; Wang, J. Passively Q-switched 1.34  $\mu\text{m}$  Nd:Y<sub>x</sub>Gd<sub>1-x</sub>VO<sub>4</sub> laser with  $\text{Co}^{2+}:\text{LaMgAl}_{11}\text{O}_{19}$  saturable absorber. *Opt. Express* **2006**, *14*, 7730–7736. [[CrossRef](#)]
97. Omatsu, T.; Miyamoto, K.; Okida, M.; Minassian, A.; Damzen, M.J. 1.3- $\mu\text{m}$  passive Q-switching of a Nd-doped mixed vanadate bounce laser in combination with a V:YAG saturable absorber. *Appl. Phys. B* **2010**, *101*, 65–70. [[CrossRef](#)]
98. Zhang, B.T.; Huang, H.T.; He, J.L.; Yang, J.F.; Xu, J.L.; Zuo, C.H.; Zhao, S. Diode-end-pumped passively Q-switched 1.34  $\mu\text{m}$  Nd:Gd<sub>0.5</sub>Y<sub>0.5</sub>VO<sub>4</sub> laser with  $\text{Co}^{2+}:\text{LMA}$  saturable absorber. *Opt. Mater.* **2009**, *31*, 1697–1700. [[CrossRef](#)]
99. Zhang, S.; Wang, X.; He, J.; Yang, Q.; Li, X.; Zhao, B. Passively Q-switched laser performance of an a-cut Nd:Lu<sub>0.33</sub>Y<sub>0.36</sub>Gd<sub>0.3</sub>VO<sub>4</sub> crystal at 1.34  $\mu\text{m}$  with  $\text{V}^{3+}:\text{YAG}$  as the saturable absorber. *Laser Phys.* **2013**, *23*, 095805. [[CrossRef](#)]
100. Li, X.; Li, G.; Zhao, S.; Xu, C.; Du, G. Diode-pumped passively Q-switched Nd:Lu<sub>x</sub>Y<sub>1-x</sub>VO<sub>4</sub> laser at 1.34  $\mu\text{m}$  with two V:YAG saturable absorbers. *Opt. Commun.* **2011**, *284*, 1307–1311. [[CrossRef](#)]
101. Cai, E.; Xu, J.; Zhang, S.; Wu, Z. Tin disulfide as saturable absorber for the 1.3  $\mu\text{m}$  nanosecond laser. *Laser Phys. Lett.* **2022**, *19*, 065802. [[CrossRef](#)]
102. Cai, E.; Xu, J.; Liu, Y.; Zhang, S.; Fan, X.; Wang, M.; Lou, F.; Lv, H.; Wang, X.; Li, T. Passively Q-switched and Q-switched mode-locked Nd:Lu<sub>0.15</sub>Y<sub>0.85</sub>VO<sub>4</sub> lasers at 1.34  $\mu\text{m}$  with a nickel-cobalt layered double hydroxide saturable absorber. *Opt. Mater. Express* **2022**, *12*, 931–939. [[CrossRef](#)]
103. Han, S.; Xu, H.H.; Zhao, Y.G.; Chen, L.J.; Wang, Z.P.; Yu, H.H.; Zhang, H.J.; Xu, X.G. The  $^4\text{F}_{3/2} \rightarrow ^4\text{I}_{13/2}$  transition property of Nd:La<sub>0.05</sub>Lu<sub>0.95</sub>VO<sub>4</sub> crystal. *Laser Phys.* **2013**, *23*, 105814. [[CrossRef](#)]
104. Guo, L.; Lan, R.; Liu, H.; Yu, H.; Zhang, H.; Wang, J.; Hu, D.; Zhuang, S.; Chen, L.; Zhao, Y.; et al. 1319 nm and 1338 nm dual-wavelength operation of LD end-pumped Nd:YAG ceramic laser. *Opt. Express* **2010**, *18*, 9098–9106. [[CrossRef](#)]
105. Jabczynski, J.K.; Zendzian, W.; Kwiatkowski, J.; Šulc, J.; Nemeč, M.; Jelínková, H. Passively Q-switched neodymium slab lasers at 1.3- $\mu\text{m}$  wavelength side-pumped by a 600-W laser diode stack. *Opt. Eng.* **2006**, *45*, 114204. [[CrossRef](#)]
106. Li, P.; Chen, X.H.; Zhang, H.N.; Wang, Q.P. Diode-end-pumped passively Q-switched 1319 nm Nd:YAG ceramic laser with a  $\text{V}^{3+}:\text{YAG}$  saturable absorber. *Laser Phys.* **2011**, *21*, 1708–1711. [[CrossRef](#)]
107. Lin, B.; Xiao, K.; Zhang, Q.L.; Zhang, D.X.; Feng, B.H.; Li, Q.N.; He, J.L. Dual-wavelength Nd:YAG laser operation at 1319 and 1338 nm by direct pumping at 885 nm. *Appl. Opt.* **2016**, *55*, 1844–1848. [[CrossRef](#)] [[PubMed](#)]
108. Podlipensky, A.V.; Yumashev, K.V.; Kuleshov, N.V.; Kretschmann, H.M.; Huber, G. Passive Q-switching of 1.44  $\mu\text{m}$  and 1.34  $\mu\text{m}$  diode-pumped Nd:YAG lasers with a V:YAG saturable absorber. *Appl. Phys. B* **2003**, *76*, 245–247. [[CrossRef](#)]
109. Šulc, J.; Jelínková, H.; Nemeč, M.; Nejezchleb, K.; Škoda, V. V:YAG saturable absorber for flash-lamp and diode-pumped solid state lasers. In Proceedings of the Solid State Lasers and Amplifiers: Photonics Europe, Strasbourg, France, 24–29 April 2004; Volume 5460, pp. 292–302.
110. Šulc, J.; Jelínková, H.; Nejezchleb, K.; Škoda, V. Nd:YAG/V:YAG monolithic microchip laser operating at 1.3  $\mu\text{m}$ . *Opt. Mater.* **2007**, *30*, 50–53. [[CrossRef](#)]
111. Feng, C.; Zhang, H.; Fang, J.; Wang, Q. Passively Q-switched Nd:YAG ceramic laser with  $\text{V}^{3+}:\text{YAG}$  saturable absorber at 1357 nm. *Appl. Opt.* **2015**, *54*, 9902–9905. [[CrossRef](#)]
112. Lin, H.Y.; Liu, H.; Zhang, S.Q. Passively Q-Switched 1319 nm Nd:YAG laser based on Co:MgAl<sub>2</sub>O<sub>4</sub> crystal. *Laser Optoelectron. Prog.* **2018**, *55*, 121404.
113. Xu, X.D.; Wang, X.D.; Meng, J.Q.; Cheng, Y.; Li, D.Z.; Cheng, S.S.; Wu, F.; Zhao, Z.W.; Xu, J. Crystal growth, spectral and laser properties of Nd:LuAG single crystal. *Laser Phys. Lett.* **2009**, *6*, 678–681. [[CrossRef](#)]



114. Liu, C.; Zhao, S.; Li, G.; Yang, K.; Li, D.; Li, T.; Qiao, W.; Feng, T.; Chen, X.; Xu, X.; et al. Experimental and theoretical study of a passively Q-switched Nd:LuAG laser at 1.3  $\mu\text{m}$  with a  $\text{V}^{3+}$ :YAG saturable absorber. *J. Opt. Soc. Am. B* **2015**, *32*, 1001–1006. [[CrossRef](#)]
115. Zhang, B.; Yang, J.; He, J.; Huang, H.; Liu, S.; Xu, J.; Liu, F.; Zhi, Y.; Tao, X. Diode-end-pumped passively Q-switched 1.33  $\mu\text{m}$  Nd:Gd<sub>3</sub>Al<sub>x</sub>Ga<sub>5-x</sub>O<sub>12</sub> laser with  $\text{V}^{3+}$ : YAG saturable absorber. *Opt. Express* **2010**, *18*, 12052–12058. [[CrossRef](#)]
116. Gao, S.; Wang, W. Thermal optical properties, Q-switching and frequency tuning of an Nd:LGGG laser based on the  $^4\text{F}_{3/2} \rightarrow ^4\text{I}_{13/2}$  transition of a neodymium ion. *Quantum Electron.* **2021**, *51*, 149–152. [[CrossRef](#)]
117. Kuwano, Y.; Saito, S.; Hase, S. Crystal growth and optical properties of Nd: GGAG. *J. Cryst. Growth* **1988**, *92*, 17–22. [[CrossRef](#)]
118. Jia, Z.; Tao, X.; Yu, H.; Dong, C.; Zhang, J.; Zhang, H.; Wang, Z.; Jiang, M. Growth and properties of Nd:(Lu<sub>x</sub>Gd<sub>1-x</sub>)<sub>3</sub>Ga<sub>5</sub>O<sub>12</sub> laser crystal by Czochralski method. *Opt. Mater.* **2008**, *31*, 346–349. [[CrossRef](#)]
119. Fu, X.; Jia, Z.; Li, Y.; Yuan, D.; Dong, C.; Tao, X. Crystal growth and characterization of Nd<sup>3+</sup>:(La<sub>x</sub>Gd<sub>1-x</sub>)<sub>3</sub>Ga<sub>5</sub>O<sub>12</sub> laser crystal. *Opt. Mater. Express* **2012**, *2*, 1242–1253. [[CrossRef](#)]
120. Wang, B.; Tian, L.; Yu, H.; Zhang, H.; Wang, J. Energy enhancement of mixed Nd:LuYSGG crystal in passively Q-switched lasers. *Opt. Lett.* **2015**, *40*, 3213–3216. [[CrossRef](#)]
121. Zuo, C.H.; Zhang, B.T.; He, J.L.; Dong, X.L.; Yang, J.F.; Huang, H.T.; Xu, J.L.; Zhao, S.; Dong, C.M.; Tao, X.T. CW and passive Q-switching of 1331-nm Nd:GGG laser with  $\text{Co}^{2+}$ :LMA saturable absorber. *Appl. Phys. B* **2009**, *95*, 75–80. [[CrossRef](#)]
122. Zuo, C.H.; Zhang, B.T.; He, J.L.; Dong, X.L.; Yang, K.J.; Huang, H.T.; Xu, J.L.; Zhao, S.; Dong, C.M.; Tao, X.T. CW and passively Q-switching characteristics of a diode-end-pumped Nd:GGG laser at 1331 nm. *Opt. Mater.* **2009**, *31*, 976–979. [[CrossRef](#)]
123. Zuo, C.H.; Zhang, B.T.; He, J.L. Passively Q-switched 1.33  $\mu\text{m}$  Nd:GAGG laser with  $\text{Co}^{2+}$ :LMA saturable absorber. *Laser Phys. Letters* **2011**, *8*, 782–786. [[CrossRef](#)]
124. Wang, Z.W.; Fu, X.W.; He, J.L.; Jia, Z.T.; Zhang, B.T.; Yang, H.; Wang, R.H.; Liu, X.M.; Tao, X.T. The performance of 1329 nm CW and passively Q-switched Nd:LGGG laser with low Lu-doping level. *Laser Phys. Lett.* **2013**, *10*, 055005. [[CrossRef](#)]
125. Wang, B.; Yu, H.; Zhang, H. Passively Q-switched 1.33  $\mu\text{m}$  Nd:LuYSGG laser with  $\text{V}^{3+}$ :YAG as the saturable absorber. *Laser Phys. Lett.* **2019**, *16*, 015801. [[CrossRef](#)]
126. Demidovich, A.A.; Shkadarevich, A.P.; Danailov, M.B.; Apai, P.; Gasmı, T.; Gribkovskii, V.P.; Kuzmin, A.N.; Ryabtsev, G.I.; Batay, L.E. Comparison of cw laser performance of Nd:KGW, Nd: YAG, Nd:BEL, and Nd:YVO<sub>4</sub> under laser diode pumping. *Appl. Phys. B* **1998**, *67*, 11–15. [[CrossRef](#)]
127. Chen, X.; Liu, J.; Yu, Y.; Li, T.; Sun, H.; Jin, G. Diode-side-pumped passively Q-switched Nd:YAP laser operating at 1.34  $\mu\text{m}$  with  $\text{V}^{3+}$ :YAG saturable absorber. *J. Russ. Laser Res.* **2015**, *36*, 86–91.
128. Ryan, J.R.; Beach, R. Optical absorption and stimulated emission of neodymium in yttrium lithium fluoride. *J. Opt. Soc. Am. B* **1992**, *9*, 1883–1887. [[CrossRef](#)]
129. Hardman, P.J.; Clarkson, W.A.; Friel, G.J.; Pollnau, M.; Hanna, D.C. Energy-transfer upconversion and thermal lensing in high-power end-pumped Nd:YLF laser crystals. *IEEE J. Quantum Electron.* **1999**, *35*, 647–655. [[CrossRef](#)]
130. Botha, R.C.; Strauss, H.J.; Bollig, C.; Koen, W.; Collett, O.; Kuleshov, N.V.; Esser, M.J.D.; Combrinck, W.L.; von Bergmann, H.M. High average power 1314 nm Nd:YLF laser, passively Q-switched with V:YAG. *Opt. Lett.* **2013**, *38*, 980–982. [[CrossRef](#)]
131. Li, H.; Zhang, R.; Tang, Y.; Wang, S.; Xu, J.; Zhang, P.; Zhao, C.; Hang, Y.; Zhang, S. Efficient dual-wavelength Nd:LuLiF<sub>4</sub> laser. *Opt. Lett.* **2013**, *38*, 4425–4428. [[CrossRef](#)]
132. Li, J.H.; Liu, X.H.; Wu, J.B.; Zhang, X.; Li, Y.L. High-power diode-pumped Nd:Lu<sub>2</sub>O<sub>3</sub> crystal continuous wave thin-disk laser at 1359 nm. *Laser Phys. Lett.* **2012**, *9*, 195–198. [[CrossRef](#)]
133. Li, J.; Vannini, M.; Wu, L.; Tian, F.; Hu, D.; Chen, X.; Feng, Y.; Patrizi, B.; Pirri, A.; Toci, G.; et al. Fabrication and Optical Property of Nd:Lu<sub>2</sub>O<sub>3</sub> Transparent Ceramics for Solid-state Laser Applications. *J. Inorg. Mater.* **2021**, *36*, 210. [[CrossRef](#)]
134. Rao, H.; Liu, Z.; Cong, Z.; Huang, Q.; Liu, Y.; Zhang, S.; Zhang, X.; Feng, C.; Wang, Q.; Ge, L.; et al. High power YAG/Nd:YAG/YAG ceramic planar waveguide laser. *Laser Phys. Lett.* **2017**, *14*, 045801. [[CrossRef](#)]
135. Grabtchikov, A.S.; Kuzmin, A.N.; Lisinetskii, V.A.; Orlovich, V.A.; Demidovich, A.A.; Yumashev, K.V.; Kuleshov, N.V.; Eichler, H.J.; Danailov, M.B. Passively Q-switched 1.35  $\mu\text{m}$  diode pumped Nd:KGW laser with V:YAG saturable absorber. *Opt. Mater.* **2001**, *16*, 349–352. [[CrossRef](#)]
136. Zolotovskaya, S.A.; Savitski, V.G.; Gaponenko, M.S.; Malyarevich, A.M.; Yumashev, K.V.; Demchuk, M.I.; Raaben, H.; Zhilin, A.A.; Nejezchleb, K. Nd:KGd(WO<sub>4</sub>)<sub>2</sub> laser at 1.35  $\mu\text{m}$  passively Q-switched with  $\text{V}^{3+}$ :YAG crystal and PbS-doped glass. *Opt. Mater.* **2006**, *28*, 919–924. [[CrossRef](#)]
137. Chen, H.; Zhou, M.; Zhang, P.; Yin, H.; Zhu, S.; Li, Z.; Chen, Z. Passively Q-switched Nd:GYAP laser at 1.3  $\mu\text{m}$  with bismuthene nanosheets as a saturable absorber. *Infrared Phys. Technol.* **2022**, *121*, 104023. [[CrossRef](#)]
138. Gao, X.; Li, S.; Li, T.; Li, G.; Ma, H. g-C<sub>3</sub>N<sub>4</sub> as a saturable absorber for the passively Q-switched Nd:LLF laser at 13  $\mu\text{m}$ . *Photonics Res.* **2017**, *5*, 33–36. [[CrossRef](#)]